THROMBOLYSIS OF BLOOD CLOTS USING WIRELESSLY POWERED INFERIOR VENA CAVA FILTERS

A Thesis
Submitted to the Graduate Faculty
of the
North Dakota State University
of Agriculture and Applied Science

By

Nolan Gregory Schwarz

In Partial Fulfillment of the Requirements
for the Degree of
MASTER OF SCIENCE

Major Program:
Biomedical Engineering

April 2018

Fargo, North Dakota

North Dakota State University
Graduate School

Title

Thrombolysis of Blood Clots Using Wirelessly Powered Inferior Vena Cava Filters

By

Nolan Gregory Schwarz

The Supervisory Committee certifies that this ***disquisition*** complies with North Dakota State University's regulations and meets the accepted standards for the degree of

MASTER OF SCIENCE

SUPERVISORY COMMITTEE:

Dr. Ivan Lima Jr.
Chair

Dr. Amanda Brooks

Dr. Mark Jensen

Approved:

4/10/2018
Date

Dr. Benjamin Braaten
Department Chair

ABSTRACT

Venous thromboembolisms (VTE) are estimated to affect up to 900,000 individuals in the U.S. each year. Traditionally, VTE is treated prophylactically with anticoagulants or directly with thrombolytic therapies. Both treatments have significant limitations, side effects, and potentially fatal adverse effects. Inferior vena cava filters are another treatment for VTE but are less common because of risks like clot accumulation and occlusion. Modifying the standard filters to wirelessly powered thrombolytic filters combines the positive attributes of anticoagulants and thrombolytics without the associated adverse effects. Computer simulations and *in vitro* experiments were conducted to assess the feasibility and effectiveness of a wirelessly powered filter. The filters are designed to capture and then heat blood clots. At 55°C the D fragment domains of fibrin denature causing the entire structure to break apart. This allows the filter to prevent formation of new clots as well as dissolve captured clots, preventing accumulation.

ACKNOWLEDGEMENTS

I'd like to begin by thanking Dr. Ivan T. Lima Jr. for the opportunity to study with him as one of the first biomedical engineering students, and for his guidance during my time as both as an undergraduate and as a graduate student.

Additionally, I'd like to thank Dr. Amanda Brooks for her significant contributions to many of the projects I have worked on with her as well as for her guidance in finding the real value in learning and as a role model. She has challenged the way I approach problems and communicate my ideas to help me grow as a scientist and person. These are skills I will always be grateful to have.

I'd also like to thank Dr. Mark Jensen for taking the time to work with engineering students to help them and myself develop skill sets to aid in solving problems in medicine as well as for his support of my current and future academic endeavors.

To my friends, who have shared in the highs and lows - I truly appreciate the many times you sacrificed to put some of my work before your own. Know that although I may not maintain contact as often as I would hope, I will always consider every one of you as my friends and will be there for anything you need from me, as you were when I needed you.

DEDICATION

To my mother, Darlene Schwarz, and father, Gerald Schwarz, who always supported me in everything I wanted to accomplish and teaching me to never give up despite adversity, all without expecting anything more than my happiness. I will never be able to properly express how grateful I am for all you do for me, and I assure you anything great I've ever done, or will do, is because of you.

And to my intelligent and beautiful fiancée Rose Hoechst, who has been the person that I most depend on and is a constant source of support and encouragement during life's challenges. I am truly thankful for having you in my life, and this work and what I hope to do would be impossible without you.

TABLE OF CONTENTS

LIST OF TABLES

LIST OF FIGURES

LIST OF ABBREVIATIONS

VTE.....Venous ThromboEmbolisms.

DVT .....Deep Vein Thrombosis

PE.....Pulmonary Embolism.

TF.....Tissue Factor.

TFPI .....Tissue Factor Pathway Inhibitor.

AT .....AntiThrombin.

UFH.....UnFractionated Heprin.

LMWH.....Low Molecular Weight Heprin.

aPTT.....active Partial Thromboplastin Time.

MI.....Myocardial Infarction.

VKA.....Vitamin K Antagonist.

INR.....International Normalized Ratio.

DOAC .....Direct Oral AntiCoagulants.

NOAC .....New Oral AntiCoagulants.

FDA.....Food and Drug Administration.

EMA.....European Medicine Agency.

GI .....GastroIntenstinal.

CrCl.....Creatinine Clearance.

IVC.....Inferior Vena Cava.

DEP .....DiElectroPhoresis.

RF.....Radio Frequency.

SAR.....Standard Absorption Rate.

FCC .....Federal Communications Commission.

ICNIRP .....International Commission of Non-Ionizing Radiation Protection.

LIST OF APPENDIX TABLES

1. INTRODUCTION

Venous thromboembolisms (VTE) are blood clots that form in the veins and are the third most common vascular disease following heart attack and stroke. VTE is broken down into two major categories: deep vein thrombosis (DVT) and pulmonary embolism (PE). DVT is the development of a blood clot in any vein, but these clots most often occur in the legs. Pulmonary embolism occurs when a DVT breaks free from the wall of a vein and travels to the lung, blocking part or all of the blood supply, which reduces the amount of oxygenated blood reaching the body, specifically the heart and brain [1].

1.1. Problem Overview

VTE is a complex disease because of the combination of inheritable predispositions towards the disease along with acquired and environmental risk factors such as advanced age, immobility, surgery, cancer, and obesity, becoming more common in the United States and around the world [2]. VTE has been categorized as a major public health problem by the U.S. Surgeon General due to the rapidly increasing incidence and cost of treatment. There are several methods of treatment for venous thromboembolism. The most common are anticoagulants such as warfarin, the number one drug causing emergency hospitalization in patients 65 and older [3], [4], and inferior vena cava filters that prove to be more risky than anticoagulants with use durations greater than a year. VTE is a rapidly growing problem that effects people in many demographics, and still has a critical need for a treatment that can improve efficacy, reduce VTE recurrence, and minimize adverse effects.

1.1.1. Disease Significance

The Center for Disease Control and American Heart Association estimate that there are greater than 900,000 Americans affected each year, with an estimated incidence of greater than

300 per 100,000 person-years, and nearly a third of these cases experience a recurrence within ten years [3], [5]. Cancer patients make up approximately twenty percent of VTE cases, and in a Dutch Cancer Registry study, cancer patients with clinical VTEs had a 2.2-fold increase in mortality than controls-matched cancer patients without VTE [6]. The one-year fatality rate among patients with cancer and VTE is 63.4% (95% CI: 54.5–71.8). In VTE cases without active cancer status, the one-year fatality rate is still high at 12.6% (n = 77; 95% CI: 10.1%–15.5) [7].

1.1.2. Economic Costs of Venous Thromboembolism

In addition to the cost of patient's health and quality of life, VTE also places a large economic burden on patients. The costs for cancer patients with VTE were 2.5-fold higher ($62,838) than for controls matched patients ($24,464) (P=<0.001). The cost differences observed were largest during the first three months, but the costs stayed significantly higher for the entire 5-year study [8]. The same was true for patients undergoing surgery; the cost was 1.5-fold higher for surgical patients with VTE ($55,956) than for controls matched patients ($32,718) (P=<0.001), and this cost stayed on average $10,797 greater for the duration of the studies [8]–[10].

2. TREATMENTS OF VENOUS THROMBOEMOLISMS

2.1. Anticoagulant Therapies

Treatment for VTE is most often anticoagulants, or blood thinners, such as warfarin (Coumadin) or rivaroxaban (Xarelto), which do not actively break apart thromboembolisms, but instead prevent the formation and growth of blood clots by blocking various steps in the coagulation cascade.

2.1.1. Coagulation System

Beginning in the 1960's, blood coagulation mechanisms started to be described as a "cascade" of enzymes activating downstream enzymes to plug wounds and stop the bleeding. This process became known as hemostasis from the Greek roots *haeme* meaning blood and *stasis* meaning stop [11]. This process can roughly be further broken down to primary hemostasis and the coagulation cascade.

Primary hemostasis is the result of platelets interacting with endothelial cell's adhesive proteins and extra cellular matrix to start the initial formation of a "platelet plug." The endothelial cells lining the blood vessels have multiple antithrombotic mechanisms; it is when the layers below the endothelium become exposed, like during vascular injury, that collagen and thrombogenic proteins are released to induce the formation of the platelet plug that serves as the scaffold for the final fibrin-platelet aggregate [11]–[13]. After a platelet adheres to the exposed collagen and releases its factors, it begins to secrete its two types of granules along with various other factors that stimulate further platelet aggregation to temporarily seal off the vascular injury and start the coagulation cascade [11].

The coagulation cascade is a complex set of interconnected reactions which result in the conversion of soluble fibrinogen to insoluble fibrin strands. Many of the clotting factor enzymes exist in an inactive form and are circulating in the blood stream (shown in Table 1).

Table 1. Coagulation proteins/ clotting factors [13].

Clotting Factor Number	Clotting Factor Name	Function	Plasma half-life (hours)	Plasma Concentration (mg/L)
I	Fibrinogen	Clot Formation	90	3000
II	Prothrombin	Activation of I, V, VII, VIII, XI, XIII	65	100
III	Tissue Factor	Cofactor of VIIa	-	-
IV	Calcium	Facilitates coagulation factor binding to phospholipids	-	-
V	Proaccelerin	Cofactor of X-prothrombinase complex	15	10
VI	Unassigned	-	-	-
VII	Stable factor	Activates IX, X	5	0.5
VIII	Antihemophilic factor A	Cofactor of IX-tenase complex	10	0.1
IX	Antihemophilic factor B or Christmas factor	Activates X; forms complex with VIII	25	5
X	Stuart-Prower factor	Complex with V; activates II	40	10
XI	Plasma thromboplastin antecedent	Activates IX	45	5
XII	Hageman factor	Activates XI, VII	-	-
XIII	Fibrin-stabilizing factor	Cross-links fibrin	200	30

The cascade of the clotting enzymes has traditionally been classified into intrinsic and extrinsic pathways which connect in a common pathway with the activation of factor X (shown in Figure 1A). These pathways provided an effective understanding of the basics of the coagulation pathway and understanding of *in vitro* coagulation tests, but these pathways do not completely explain the *in vivo* pathway. One example is a deficiency of factors VIII and IX; both factors are involved in the intrinsic pathway and cause hemophilia A and B respectively, but these disorders do not allow the blood to clot via the extrinsic pathway either. Instead of two

parallel pathways, the current coagulation concept used (shown in Figure 1B) is described with three phases: initiation, amplification, and propagation [12], [13].

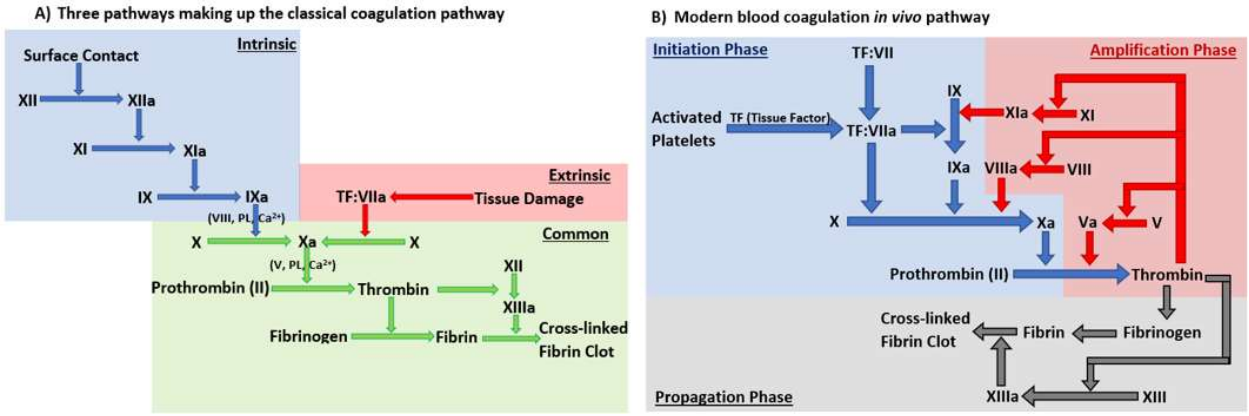

Figure 1. 1A) The traditional coagulation pathway and 2B) a modern interpretation of the coagulation cascade pathways. Figures adapted from [14].

Initiation starts when tissue factor (TF), expressed on the surface of cells that are not in contact with the blood, is exposed to the circulating or released clotting factors. TF quickly binds to factor VII to form the TF-VIIa complex, which in turn binds with factors IX and X to form prothrombinase complexes. The formation of these complexes occurs on the cells where TF factor was initially bound, but the converting of trace amounts of prothrombin to thrombin starts the amplification step and generation of the complexes on the platelet surfaces that will form the bulk of the clot [11]–[13], [15].

Amplification is a positive feedback loop where Thrombin activates factors XI, VIII, and V starting the buildup of more prothrombinase complexes. The enzyme complexes generated during amplification, such as factor VIII, mediate platelet activation and adhesion to allow the accumulation of complexes on platelet surfaces to support the continued production of thrombin and fibrin during the propagation phase [11]–[13], [15].

The propagation phase is distinguished by the large-scale cleavage of fibrinogen into fibrin and the polymerization of the fibrin with activated platelets into the platelet plug. Once the platelet plug is formed and the lesion sealed, termination of the positive feedback loop and clotting process begins [11]–[13], [15].

After the clot has formed at a vascular lesion, termination begins by releasing four natural anticoagulants to prevent the occlusion of the vessel due to excess thrombotic activity. The four natural anticoagulants are tissue factor pathway inhibitor (TFPI), antithrombin (AT), protein C, and protein S. TFPI binds to the TF-VIIa prothrombinase complex, which inactivates the factors and the complex [13]. AT inhibits the activity of thrombin as well as the other serine protease factors Xa, XIa, and XIIa. Epithelial cells produce several surface proteins with a high affinity for AT as one natural mechanism to prevent the spontaneous formation of thrombus formation as well as terminate the coagulation pathway. Protein C and S both terminate the clotting process by inhibiting factors Va and VIIIa, two of the major factors in amplification and propagation. Protein C is located on the surface of epithelial cells and is activated by thrombin. Protein S is also located on epithelial cell membranes, but nearly a third of protein S exists as a free protein in circulation [12], [13]. The balance between coagulation and anticoagulation is a difficult and complex process for the body, but with a better understanding of this balance, the methods for treating these imbalances will be more meaningful.

2.1.2. Heparin

Heparin, one of the first anticoagulants, is a naturally occurring glycosaminoglycan. Heparin is still heavily in use today despite being discovered in 1916, and is listed as one of the World Health Organization's List of Essential Medicines [15]. Heparin is used in two forms: a standard or unfractionated heparin (UFH) or a low-molecular weight heparin (LMWH), which is

prepared by depolymerization and weight separation. The LMWH has shown to be at least as safe and effective as unfractionated heparin when UFH is administered by continuous intravenous infusion and dosage carefully monitored to keep the active partial-thromboplastin time (aPTT) within therapeutic range. The LMWH can be more conveniently administered by subcutaneous injection in doses adjusted for patient weight and does not need the aPTT monitored [16]. This is possible because not all heparin molecules have the same anticoagulant properties.

Heparin is a chain composed of alternating residues of D-glucosamine and uronic acid, but approximately one third of the molecules also contain a unique pentasaccharide that gives the molecule a high affinity for binding and antithrombin [17]. This bond is the primary mechanism for heparin's anticoagulation properties and allows the more active molecules to be separated out by molecular weight. Heparin causes a conformational change that dramatically increases the reaction rate of antithrombin and therefore inactivation of thrombin.

The direct increase in activity of antithrombin and the rapid therapeutic onset after administration make heparin and lovenox/enoxaparin (brand/generic for LMWH) a great choice for its many indications: Prophylaxis of DVT and PE, as a bridge treatment with warfarin, prophylaxis of non-Q wave myocardial infarction (MI), and treatment of acute ST-segment elevation MI [18].

LMWH and UFH are more commonly used with inpatient healthcare and in finite durations due to many patients not being comfortable with regular or daily intravenous or injection treatments. The long term usage of heparin also brings the risk of thrombocytopenia (moderate disease is a platelet count of >50,000/μl and <100,000/μl), which occurs in 1.3% of patients [18]. Elevated levels of serum aspartate and alanine aminotransferases have also been

shown to be elevated in as many as 80% of patients and above the laboratory upper limit reference range in up to 6.1% of patients [18], [19]. For these reasons, Heparin is still an important and highly utilized option for anticoagulation and treatment of VTE, but a treatment that can be safely used for years without reducing a patient's quality of life would prove to be a better option.

2.1.3. Vitamin K Antagonists

Vitamin K antagonists (VKA) are a class of oral anticoagulants that have been the primary means of VTE anticoagulant treatment for sixty years. It was very quickly accepted due to its high bioavailability when taken orally, dramatically improving quality of life for patients, and its clinically proven effectiveness [20].

The mechanism of action in VKA is to inhibit the activity of the enzyme vitamin K epoxide reductase, which is responsible for converting the inactive oxidized form of vitamin K into the active reduced form (shown in Figure 2). The active form is a cofactor for the posttranslational modifications that need to be made to the coagulation factors before they are functional. When this process is inhibited, the availability of active vitamin K drops, which leads to a drop in the amount of functional coagulation factors II, VII, IX, X and results in reduced clotting ability [20]. This action of reducing the available functional and active factors is one of the reasons vitamin K antagonists like warfarin need a few days to reach therapeutic levels. The most common of the vitamin K antagonists is warfarin, which is often used in conjunction with LMWH to bridge the nontherapeutic period [20]. Bridging is important because the natural anticoagulation factors, proteins C and S, are also vitamin K dependent, so initially vitamin K antagonists like warfarin can result in a hypercoagulation state instead of the desired anticoagulation state.

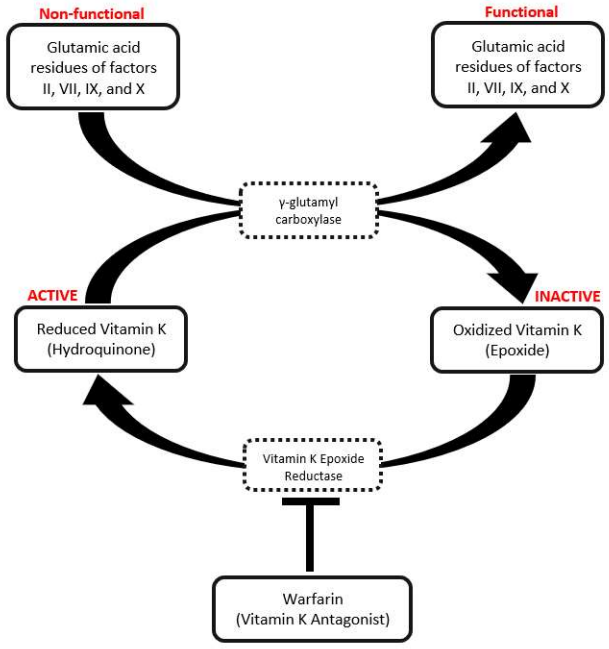

Figure 2. Mechanism for the vitamin K dependent step of synthesizing some of the coagulant factors, and the inhibition of this process by warfarin or any vitamin K antagonist.

Warfarin and other vitamin K antagonists have proven to be effective for their specific indications such as prophylaxis and treatment of venous thrombosis and pulmonary embolism, prophylaxis of atrial fibrillation or valve replacement thromboembolic complications, and reduction in risk of myocardial infarction, stroke, and systemic embolization [21]. Over time, the adverse effects and limitations started to appear. The limitations encountered in clinical practice are 1) VKA's have a narrow therapeutic window, 2) the dosage necessary has considerable variability from patient to patient, 3) VKAs interact with diets and other therapies, 4) maintenance of therapeutic levels requires a solid understanding of the pharmacokinetics and dynamics along with regular and helpful patient communication [20].

Oral warfarin has a very narrow period in which its anticoagulation effect is at an ideal level (INR between 2 and 3). The onset of action for oral warfarin sodium is 24-72 hours, but full therapeutic effect is not reached for 5 to 7 days. This again is why bridging is needed for patients at immediate risk for thrombotic injury. Patients are also at risk for the adverse effects associated

with warfarin; this also means that patients need to have the dosage carefully monitored to maintain a safe coagulation state [21].

Monitoring and choosing safe dosages for patients is also made difficult by the fact that effective dosages vary widely between patients. Warfarin is a racemic mixture where the S enantiomer, which is 3 to 5 times more active, is metabolized in the liver by the CYP2C9 enzyme of the cytochrome P450 system. The R enantiomer is also metabolized in the liver, but is instead metabolized by the 1A2 and 3A4 enzymes [22]. The P450 CYP2C9 enzyme responsible for the metabolization of the more active enantiomer has two common and well documented alleles, 2C9*2 and 2C9*3, which are associated with impaired metabolism and an increased half-life and reduced elimination of warfarin. The VKOR gene, the gene coding for vitamin K oxide reductase, has also been found to have several mutations that confer some resistance to VKAs to individuals [23]. It has also been shown that adverse clinical outcomes using warfarin are associated with both of these mutations [24]. Choosing the correct initial dosage is important and can be made easier by the prescribing information in Table 2, but there are still many other factors that need to be considered because of the many associated interactions with VKAs.

Table 2. Ranges of expected warfarin daily doses based on genotypes [23].

VKORC1	CYP2C9					
	*1/*1	*1/*2	*1/*3	*2/*2	*2/*3	*3/*3
GG	5-7mg	5-7mg	3-4mg	3-4mg	3-4mg	0.5-2mg
AG	5-7mg	3-4mg	3-4mg	3-4mg	0.5-2mg	0.5-2mg
AA	3-4mg	3-4mg	0.5-2mg	0.5-2mg	0.5-2mg	0.5-2mg

Therapeutic dosages are also difficult to maintain due to the many interactions with diet and other drugs. The effects of vitamin K antagonists are dependent on reduced concentrations of the active vitamin K. If a substantial amount of vitamin K is ingested, such as in the leafy greens

of a salad, this could increase the concentration of vitamin K and the production of functional coagulation factors [24]. Drugs also increase and decrease the pharmacodynamics of warfarin. Drugs that inhibit the clearance of S-warfarin and increase its anticoagulant effects are phenylbutazone, metronidazole, and trimethoprim-sulfamethozazole. Drugs like barbiturates, rifampin, and azathioprine all increase hepatic clearance and therefore inhibit the anticoagulant effect [25]. There are nearly 150 drugs and numerous supplements and foods that have known interactions with warfarin. These interactions increase patient complications and make management more difficult on healthcare professionals and patients [20].

The maintenance of dosages and the amount of communication required between providers and patients is another barrier to effective VKA treatment. For maintenance to occur, patients need to be honest about their lifestyle, diet, and adherence to the prescribed dosages. Even with objective INR measurements, if the patient is not complying or being honest with the provider, INR values could vary dangerously in both directions. High risk for non-compliance is a listed contraindication for warfarin. Patients are often scheduled to come in every week to every month depending on INR consistency to check their INR values. These regular visits can become difficult for patients, especially the elderly, when making travel arrangements that change times and frequency. The regular adjustment of dosages can also make patients skeptical of providers, and again with the elderly, can make compliance difficult.

Despite several major limitations, vitamin K antagonists like warfarin have proven to be effective for their designed purpose with the benefits often outweighing the risks. This has not stopped scientists from attempting to develop better options, such as next generation of anticoagulants with a more direct mechanism of action to minimize the number of interactions and unforeseen side effects.

2.1.4. Direct Acting Oral Anticoagulants

Direct acting oral anticoagulants were previously known as new or novel oral anticoagulants (NOAC) and have only been available since the late 2000's with only five currently approved (apixaban, betrixaban, dabigatran, edoxaban, and rivaroxaban).

This class of drugs has become widely used because of their high oral availability and distinct advantages over the most common anticoagulation option, warfarin. The first advantage being that no maintenance labs are required of patients. The drugs are typically a once or twice daily by mouth fixed dosage determined by indication, age, creatinine clearance, and body weight [26]–[29]. This is possible because DOACs have better understood mechanisms with more predictable Pharmacokinetics and dynamics than VKAs like warfarin.

Apixaban, edoxaban, and rivaroxaban fall into a subclass of DOACs called direct factor Xa inhibitors. As opposed to VKAs like warfarin, direct factor Xa inhibitors block the activity of only a single factor in the coagulation cascade. Rivaroxaban was the second direct oral anticoagulant approved by the FDA and European medicine agency (EMA) and is a competitive, dose-dependent, inhibitor of factor Xa [30]. It is rapidly absorbed and reaches peak plasma concentration in less than four hours. About a third (35%) of Rivaroxaban is excreted through renal clearance with the other two thirds being metabolized in the liver by CYP3A4 and 2J2 enzymes of the P450 system. Concomitant treatment with P450 isozymes and P-glycoprotein inhibitors are therefore contraindicated due to the increased risk for bleeding [31]. Rivaroxaban is also contraindicated for patients with extreme renal impairment. A long term double bind follow-up study called the ROCKET AF was conducted to assess rivaroxaban's efficacy compared to dose adjusted warfarin. The study found that there were no significant differences in risk of major bleeding or mortality. Intracranial and fatal bleeding were less common with using

rivaroxaban, but there were more incidents of gastrointestinal bleeding and transfusion [32], [33].

Apixaban and edoxaban are reversible direct factor Xa inhibitors that function very similarly to rivaroxaban. They both have a slightly faster time to maximum plasma concentration of one to four hours. Apixiban is primarily metabolized in the liver (25%) like rivaroxaban, while edoxaban is excreted half by the liver and half in the renal system. The long-term study for apixaban showed the same efficacy as warfarin with a clear reduction in the number of intracranial bleeds and major hemorrhages. Apixaban did not have the rise in gastrointestinal bleeding that is seen with the other DOACs. Edoxaban is FDA approved but has not yet been approved by the EMA, and due to its higher renal clearance, is contraindicated for patients with creatinine clearance <50ml/min.

Dabigatran falls into the other category of DOACs, the direct thrombin inhibitors. Dabigatran was the first of the DOACs to be studied for long term efficacy and approved by the FDA [30]. It is an orally administered inactive drug, which is activated in the body by an esterase-mediated conversion where it becomes a highly specific competitive inhibitor of activated thrombin (IIa). It has an onset of action of one to two hours and reaches peak plasma levels in two to three hours. Direct thrombin inhibitors have no major food interactions and a low number of drug interactions [30]. In subsequent studies dabigatran has proven to be non-inferior to warfarin for most indications with the additional benefit of reduced risk of ischemic stroke, intracranial hemorrhage, and mortality, but with an increased risk for major GI bleeding [36]. Dabigatran is primarily excreted through the renal system (80%) and is generally contraindicated for patients with reduced kidney function (CrCl <50ml/min; CrCl >60ml/min is considered acceptable kidney function by most guidelines). There has been a halved dosage approved by the

FDA, and NOT the EMA, for a creatinine clearance of greater than 15ml/min but less than 30ml/min [30].

These pharmaceutical therapies have many mechanisms of action to treat VTE with a high level of efficacy, but both the older treatments, like heparin and warfarin, as well as the new direct oral anticoagulants have several major limitations that are acceptable because of the large risk associated with untreated VTEs. These limitations include adverse effects such as major hemorrhage (5-6%), wound secretion (3%), and neuromuscular/skeletal pain (1-4%) as well as the numerous contraindications, drug and diet interactions, and complex treatments for patients to follow [21], [31]. These pharmaceutical treatments provide high efficacy, but circulating medication inevitably leads to unpredicted affects. This expands possible treatments to mechanically designed devices.

2.2. Inferior Vena Cava Filters

2.2.1. History of Inferior Vena Cava Filters

The history of Inferior Vena Cava (IVC) interruptions to attempt to capture blood clots include a wide variety of innovations and devices, but today's IVC filters are almost all designed around the original Greenfield filter developed in 1973 [35]. The filter, shown in Figure 3A, has a slender conical shaped to efficiently trap and pack blood clots in the center. The filter was designed in a way that allows 70% of the volume of the filter to be filled while only blocking 50% of the cross-sectional area of the blood vessel. Theoretically, holding the clot in the center of the vessel would allow for the least disrupted uniform flow of blood, filled with natural anticoagulants, to pass over the clot and filter with some fibrinolytic activity.

Most filters developed after the original Greenfield have followed the original conical design for a base, but they have added substantial changes in geometry to reduce the minimal

size of clots that can be captured and increase retention volume while reducing obstruction to blood flow. Different materials and geometries also allow for easier implantation, indwell, and removal have also been tested. Several of these designs are shown in Figure 3.

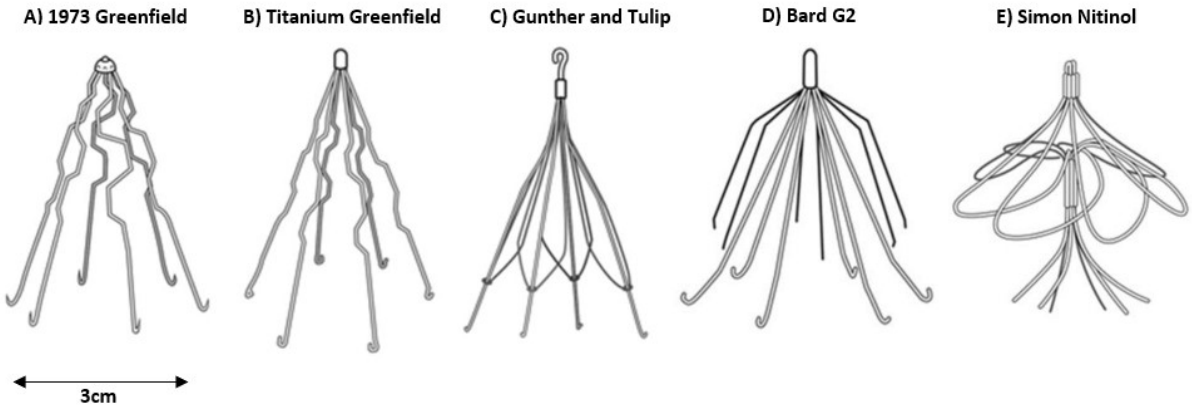

Figure 3. Depiction of five of the most common IVC filters: A) The stainless-steel Greenfield filter, B) The modified-hook titanium Greenfield filter, C) The Gunther and Tulip filter D) The Bard G2, and E) The Simon nitinol filter [36], [37].

Originally many of these filters were designed to be permanent, but these types of filters have been subjected to controversy about how safe they are for long-term use and form insertion.

2.2.2. Inferior Vena Cava Filter Implantation

Emergent placement (within the first 12 to 24 hours) of IVC filters is usually indicated for patients with 1) an acute PE or iliofemoral DVT with a contraindication for oral anticoagulation or 2) the VTE is a recurrent event despite oral anticoagulation. This emergent treatment is necessary because the mortality of recurrent PE is reported to be as high as 26%, and this highly lethal recurrence happens within 24 hours for one third of patients [38]. Patients are placed in a supine position with the head elevated 15 to 30 degrees (Trendelenburg position) to cause distention of the femoral vein and avoid the introduction of air into the venous system.

An 18G entry needle is used with a 3mm j-tipped guidewire to access the right femoral vein. Correct position of the wire is verified using ultrasonography. The needle is changed out

for an 8F sheath where the approximately 60cm 5F or 6F wire catheter is inserted over the j-tipped guide wire. The j-tipped wire is then exchanged for a 180cm stiff guide wire to insert and place the IVC filter. Proper placement of the filter is superior to the confluence of the common iliac veins and inferior to the more inferior of the two renal veins. A 12.5 MHz ultrasound probe guides this process. To deploy the IVC filter the 8F sheath is exchanged for a 12F introducer sheath and activated following the manufacture guidelines for the filter being used. There has been significant controversy about the safety of the IVC placement and deployment, but most incidents seem to occur when the filters are deployed in the hepatic or renal veins. The filters can often appear correctly placed, less than 15 degrees of tilt, even when placed in the hepatic or renal veins when only viewed from a single axis. With multi-planar imaging and insertion, deployment complications have been significantly reduced.

2.2.3. Inferior Vena Cava Filter Function

The indications for these filters are 1) recurrent embolism despite anticoagulation, 2) diagnosed DVT or PE and a contraindication to anticoagulation, 3) chronic or recurrent pulmonary embolism with associated pulmonary hypertension and cor pulmonale, 4) period following massive pulmonary embolism, 5) diagnosed DVT and a complication forcing discontinuation of anticoagulation. The only contraindications are patients with an IVC diameter of greater than 28mm (usually patients with heart failure) and the presence of a thrombus, detected and assessed by ultrasound, that risks dislodgment during the insertion procedure.

This combination of indications and contraindications would suggest that long-term usage for a patient with a strong contraindication to anticoagulants would make the Greenfield filter a good option, but research seems to suggest IVC filters are only a good short-term (less than two years) option. The median time before filter retrieval is 1.9 months (25th percentile, 1.2

months; 75th percentile, 3.2 months; range: 0-108.3 months) [39]. This is because although the filters are very effective at first when reducing the risk of pulmonary embolism by 78% ($p = 0.03$), over time the large surface area of the filters becomes the site of endothelial cells and scar tissue accumulation, foreign body granuloma formation, and the start of small thrombi. These debris impede blood flow and place additional stress on the device and vessel walls increasing the risk for VTE recurrence, device fracturing or failure, and blood vessel puncture. At two years after insertion, there is a non-significant reduction of risk for PE and the risk for DVT recurrence increases by nearly 2 fold ($p = 0.02$) [40][41].

3. APPROACHES CONSIDERED

Venous thromboembolisms are a disease with immense personal importance, and because of this, breaking apart blood clots was the goal before any idea for a solution existed. In the initial stages of this project, the idea was to use electrical or biomedical engineering techniques to improve on the IVC filters due to their high efficacy and flaws. Several ideas for improving the filters were considered and analyzed until one was chosen.

3.1. Dielectrophoresis

The first method considered as an option for improving the IVC filters was to use dielectrophoresis. Dielectrophoretic (DEP) forces work by taking advantage of the difference in electrical permeability between a particle and the solution. The idea is that there is an ideal electric field frequency that can be applied to induce a dipole in the particle that is antiparallel to the charge of the solution. The electrostatic forces then push and pull the particle through the solution. This technique is used to sort platelets out of blood and target small molecules out of solution [42]. The initial idea was to use DEP forces to pull apart the platelets and fibrin making up the clot. Following a literature search and talking with students who have used DEP with their work, it was determined that the forces generated by dielectrophoresis would not be strong enough to break the covalent bonds holding the major structures together.

3.2. Ultrasound

The next method I investigated for the mechanical breakdown of the clots was ultrasound. When reviewing the literature, several articles focus on the mechanism of how high intensity focused ultrasound works to destroy, usually cancerous, tissue. Ultrasound refers to mechanical vibrations (>16 kHz) generated by applying an alternating potential across a piezoelectric material. This material oscillates in thickness at the same frequency as the input

signal, resulting in propagating waves that cause alternating cycles of increased and reduced pressure. Based on the shape of the transducer, waves can be focused to ablate tissue at an exact point by the compression and rarefaction forces. The area of ablation is typically 1-3mm wide by 8-15mm in the direction of the wave [43].

3.3. Radio Frequency Wave Heating

The next approach that was investigated was the thermal denaturation of fibrin. The denaturation points of fibrin/fibrinogen were analyzed using absorption spectroscopy [44]. Using this technique, the authors determined that the D-domains of fibrinogen denature at ~55°C and the E-domain denatures at ~90°C. A loss of functionality would occur after the first denaturation point and lead to the destruction of the clot. Implementing the heat source in a safe manner became the next objective.

It was determined the best method to introduce this heating would be to modify an existing IVC filter by using an energy harvesting circuit and antenna to gather energy wirelessly transmitted to the filter and use it to generate a current and resistive heating.

This approach was changed slightly when it was determined a circuit harvesting a specific wavelength was unnecessary, and the stainless steel used in the filters has sufficient conductivity to use the filter itself as the antenna. These two facts allowed the circuitry to be simplified to only a power resistor designed to dissipate heat from a source frequency that has a one-half wavelength equal to the largest width of the IVC filter.

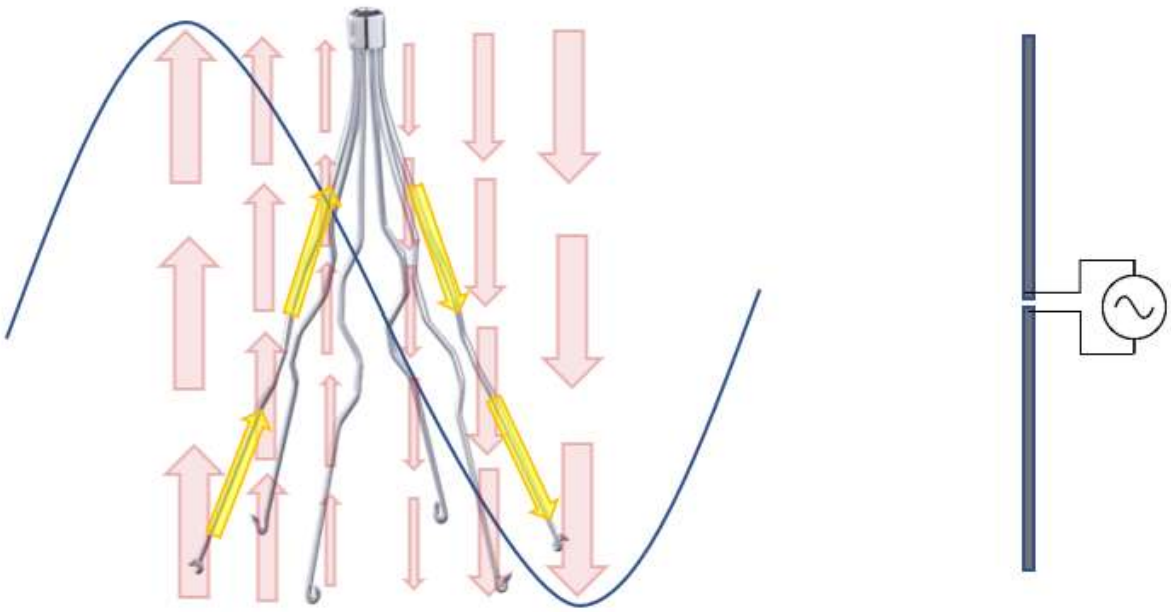

Figure 4. Propagating wave (blue sine wave) generated by the dipole antenna, the corresponding electric field vectors (red arrows), and the induced current path (yellow arrows) [45].

4. TRANSMITTING ANTENNA AND RECEIVER ORIENTATION

A large component of the vision for the final design of this project is for the filter's maintenance to be conducted by the patients in their own homes. To make this possible, the transfer of energy to the filter must be optimized to radiate the minimum energy required for operation and have the maximum amount of energy received by the filter. This depends heavily on the orientation.

4.1. Filter Orientation

Normally the position of both the transmitting and receiving antennas can be modified to fit the requirements needed to operate most effectively, but in this situation, the position of the receiving antenna is fixed by the inferior vena cava anatomy and is critical for efficacy as a blood clot filtering device. This means that all future discussion on orientation will use the filter as a fixed point with the transmitting antenna being able to move in 3-dimensional space around the IVC filter.

4.2. Excitation Wave and Filter Spatial Orientation and Optimization

Most inferior vena cava filters have significant symmetry around the same axis as the direction of blood flow in the vena cava or in the z-axis. To simplify the computer simulations the filters were simplified into an upside down 'V' shape that represents one plane of the symmetry (shown in Figure 4A as an upright 'V' shape).

The first objective in the optimization process was to determine from which direction the electromagnetic wave should approach the filter. According to reciprocity theorem of electromagnetics, the transmitting radiation pattern is the same as the receiving radiation pattern. Using MATLAB's antenna package, the 'V' shape filter was excited using a current source and the radiation pattern seen in Figure 5B was generated. This radiation pattern shows that the most

power is radiated out in the same plane as the filter perpendicular to the z-axis. It can be inferred from reciprocity theorem that this is also the best angle for the wave to approach the filter.

This finding means that the transmitting antenna must be placed at the same height as the filter. Anatomically, the antenna would be placed on the abdomen, obliques, or the lower back. Based on that anatomy, the lower back would be the best choice because the distance between the inferior vena cava and the antenna would be the lowest of the three options. Transmitting from the lower back also means the intestinal contents, which would have high variability from person to person and even time to time, would be avoided. Fewer organs between the filter and transmitting antenna also means reducing organ exposure to the RF radiation.

The next objective was determining if the angle between the legs of the 'V' shape filter influenced the efficiency of the energy transmitted to the filter. The incident wave was simulated using a plane wave, which has a uniform strength across the entire plane to give an ideal result unaffected by imperfection in the transmitting antenna. In this simulation, it was found that as the angle between the arms closed from a maximum of about 36 degrees to a minimum of 18 degrees the energy transfer efficiency dropped a small amount. The 18-degree angle would be the approximate angle corresponding to the diameter of a vena cava in the bottom 10% of vena cava size, and an appropriate energy transfer was maintained with this reduced angle.

The frequency was easily optimized once the orientation was understood. Referring to Figure 4, the excitation wave's wavelength needs to be twice the width of the 'V' shape's widest point. A wavelength of twice the width of the filter causes the two largest and opposite sign components of the wave to line up with each end of the filter. This creates a potential difference in the two arms and starts a flow of electricity through the resistive heating element at the vertex of the filter.

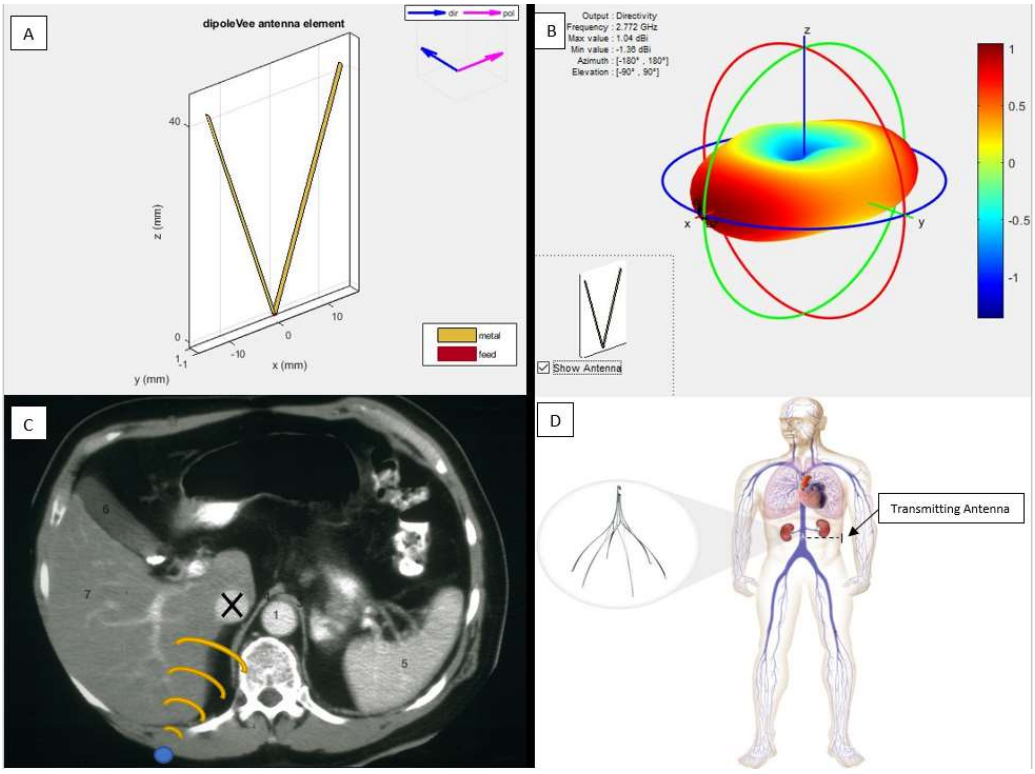

Figure 5. Figure 5A shows the V-shaped dipole generated in MATLAB is roughly the same size and shape of one arch found in an IVC filter. Figure 5B shows the radiation pattern of the antenna shown in Figure 5A. Figure 5C shows the orientation of transmitter and filter in the transverse plane. Figure 5D shows the height at which the transmitter should be placed to be level with the filter.

5. COMPUTER SIMULATIONS

The primary methods for investigating the feasibility of using a wirelessly powered IVC filter as a treatment for VTE were computer simulations. Due to the time constraints and the limited information available for this significantly different approach, computer simulations became one of the best methods for collecting useful information.

5.1. COMSOL Simulations of The Single-Plane 'V' Shape

The first simulations conducted were of the single-plane 'V' shape used earlier because of the significant reduction in the number of required meshes and, by extension, computation time.

5.1.1. Partial Filter in Air Simulations

The first simulations were conducted with the transmitting antenna and 'V' shaped filter receiving antenna in air, which has a relative permittivity and permeability equal to one. This meant that the 'V' shape filter was the only object or material interacting with the transmitted wave and would provide a coupling efficacy between the transmitter and filter based only on the orientation and design of the two antennas.

Once the geometry was designed in COMSOL's radio frequency module the first goal was characterizing how the rotation of the 'V' shape changes the amount of energy received. The calculations for the maximum energy transfer were done with the plane of the 'V' shape and the direction of the propagating wave occurring in the same direction.

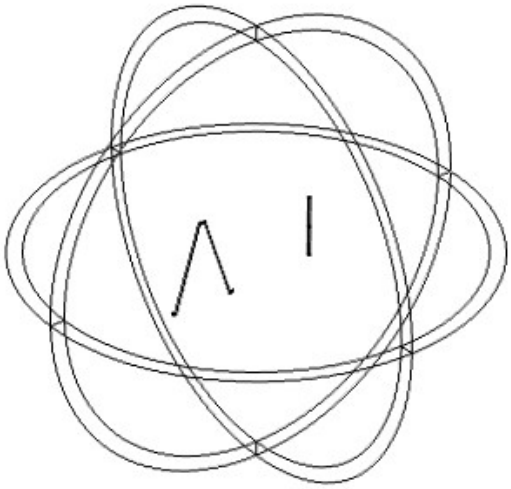

Figure 6. Wire rendering of the in-air simulation of the ‘V’ shape filter and dipole transmitting antenna.

The completed simulation (shown in Figure 6) resulted in a 9.31% energy transfer to the ‘V’ shape representing the maximum vena cava diameter of 3cm and 5.8% for the smallest simulated diameter of 1.5cm. The plots for the transmission efficiency vs the angle of the filter (0° in the figures is the plane is perpendicular to the wave direction and 90° is parallel to the wave direction) shown in Figures 7D and 7H [46].

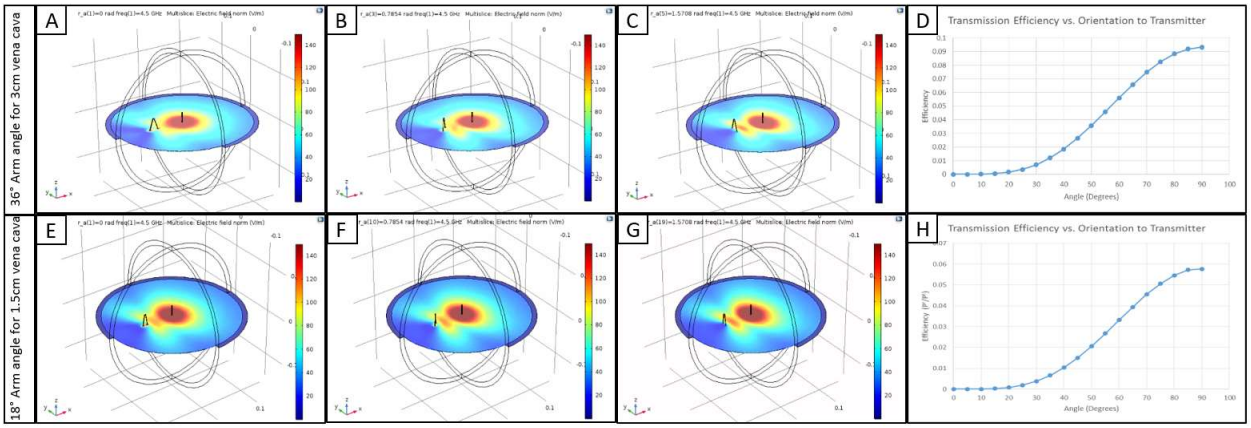

Figure 7. Figure 7A, B, and C depict the electric field plot as the 3 cm filter rotates from 90° to 0° respectively. Figure 7D is a plot of the power transfer efficiency at each angle of rotation for the 3 cm filter. Figure 7E, F, and G depict the electric field plot as the 1.5 cm filter rotates from 90° to 0° respectively. Figure 7H is a plot of the power transfer efficiency at each angle of rotation for the 1.5cm filter.

Understanding how the rotation angle affects the energy transfer provides some insight into how the full 6-legged filter might behave. If the full filter is thought of as three 'V' shape filters at three different rotation angles, the filter is composed of three arches or six arms symmetrically spread with 60° of separation between arms. This means that the three arches can be aligned with the transmitter at [60°, 60°, and 0°] or [90°, 30°, and 30°] in the two extreme cases (Figure 8). The receiver-transmitter orientations at 90°, 60°, 30°, and 0° have 9.31%, 5.60%, 0.7%, and 3.01×10^{-6}% efficiency, respectively. This gives the [60°, 60°, and 0°] filter an approximate total efficiency of 11.2%, and the [90°, 30°, and 30°] filter an approximate total efficiency of 10.71% [46].

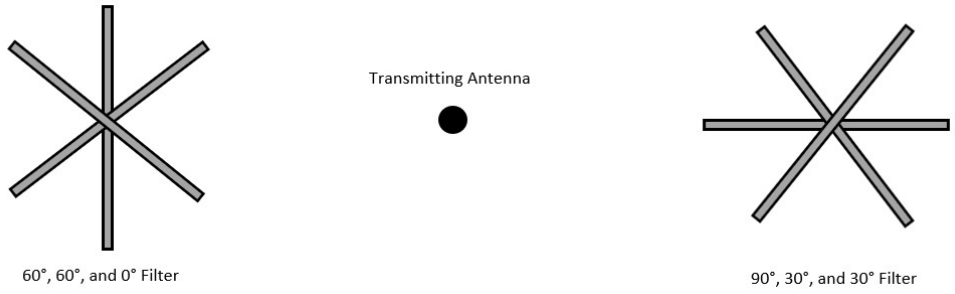

Figure 8. Top view depiction of the two orientations of the filter with transmitting antenna.

After the energy transfer efficiency with the geometry and rotation was characterized, the COMSOL microwave heating module was added to simulate the heat produced in the filter. The first simulation of temperature had a 15 W input into the transmitting antenna; the result of this input is shown in Figure 9. The apex of the filter rose to 314.45 K in less than one minute. After about 5 minutes, the temperature reached 315.10 K. Then, a 10-minute period was needed for the temperature to reach 315.20 K. Assuming a linear power/heating relationship, the input power was increased by a factor of three to 45 W to achieve the desired heating from 310 K body

temperature to 328 K. This system reached the steady state temperature of 325.10 K after about 5 minutes. Even though this system did not reach the target temperature of 328 K, the temperature 325.10 K was reached with only one of the three arches. The full system with three arches would likely exceed the denaturing temperature at 45 watts, so a lower power can be used at the transmitter [46].

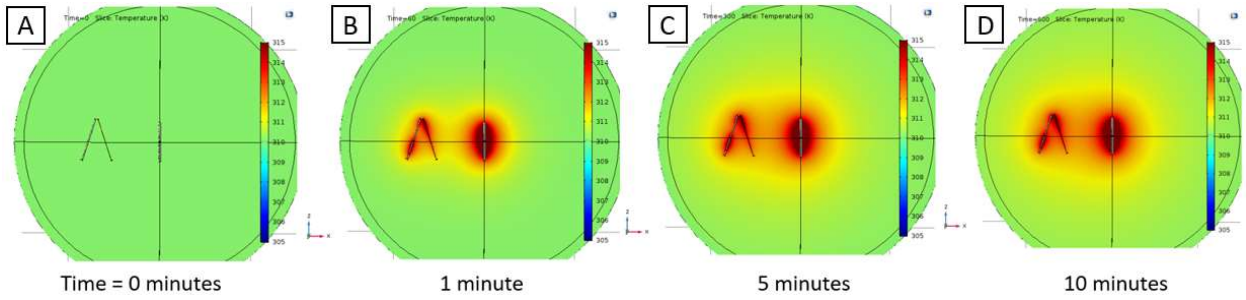

Figure 9. Figures 9A, B, C, and D are heat map plots at time 0, 1, 5, and 10 minutes after resistive heating began.

5.1.2. Partial Filter with Tissue Simulations

In the next stage of simulations, the same COMSOL radio frequency and microwave heating modules were used for the simulations with the addition of geometry that mimics the anatomy of the body (Figure 10).

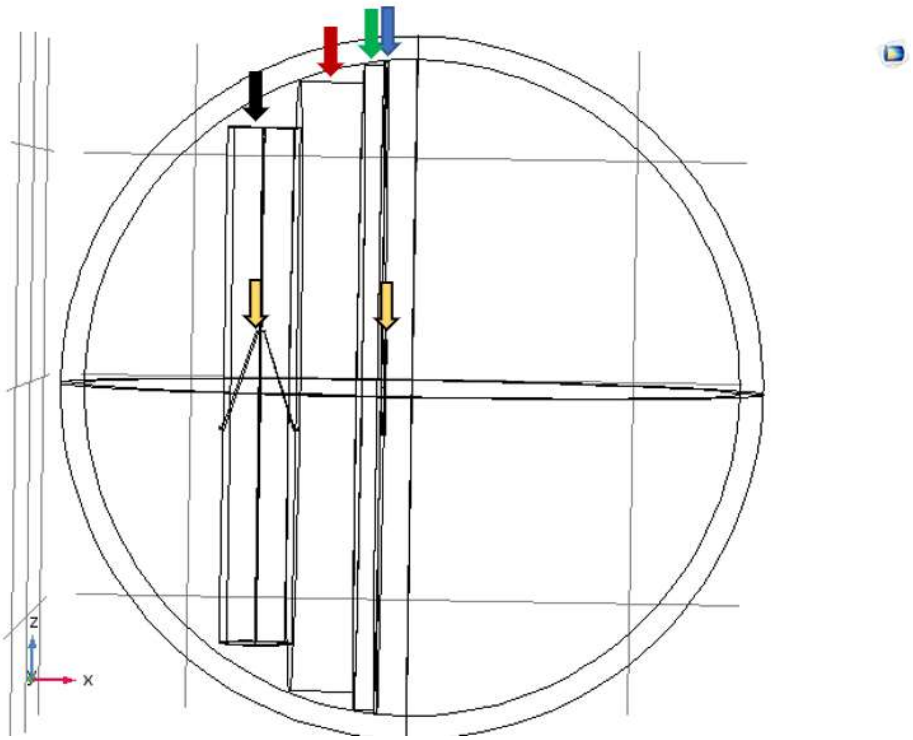

Figure 10. Wire rendering of simulation geometry with the anatomy included. The filter and the dipole antenna are shown under the yellow arrows. The inferior vena cava filled with blood is under the black arrow and around the IVC filter. The muscle, adipose, and skin layers are shown with the red, green, and blue arrows respectively.

In the first anatomical simulations, the results showed that very little of the energy was transmitted to the filter (<0.000001%). When the plot was changed to show where the power was being dissipated, Figure 11 shows that most of the power is being absorbed in the skeletal muscle. Skeletal muscle has a very high permittivity value of 50.122 compared to other tissues like adipose with a permittivity of 5.07 [47] [48]. This high permittivity rapidly diminishes the electric field and the ability of the source to power the filter.

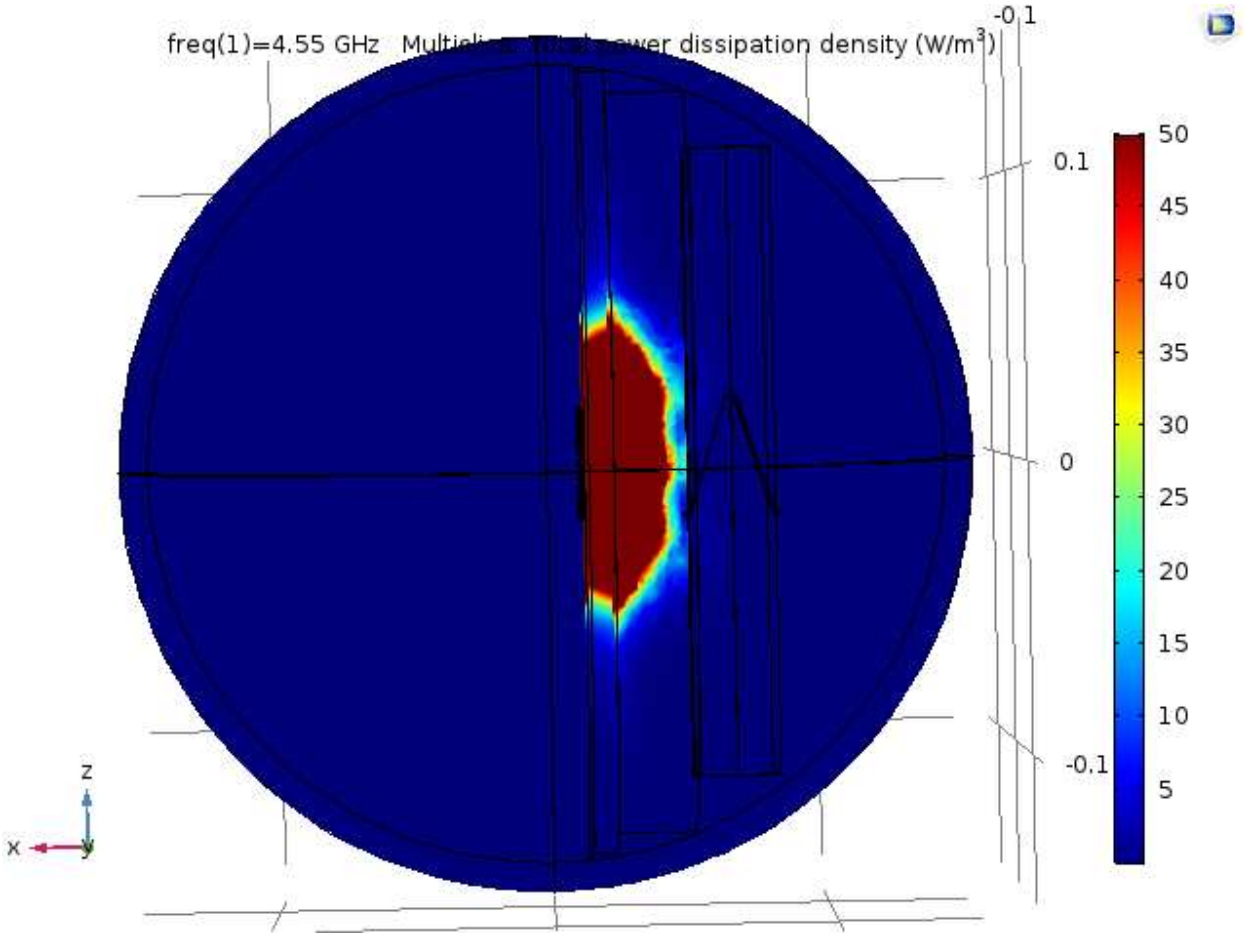

Figure 11. Power dissipation in the anatomical model (W/m^3).

The relative permittivity of the body tissues also influences the wavelength. This creates a significant problem because as the wave passes through the various body tissues the wavelength is changed and leads to a mismatch between the wavelength and filter width. The correct wavelength could be determined by a high resolution (increments of 10MHz) frequency sweep over several gigahertz, but the available computing power only allows for one frequency to be simulated at a time, each taking several hours, and no frequencies greater than 6.5GHz to be simulated. The experimental testing equipment only allows up to 3GHz to be tested.

5.2. Full IVC Filter Simulations

The next stage in the simulations were centered around the entire IVC filter. These simulations are more representative of what would likely be seen if these specific experiments were conducted, but due to the large size of the files, full frequency sweeps, characteristic impedance matching, and multiple filter sizes were not able to be completed.

5.2.1. IVC Filter in Air Simulations

The in air, full IVC filter, simulations consisted of the same dipole transmitting antenna, power radiated, separation distance, and size of simulation space. The relative permittivity and permeability equal to one in the air again helps to better understand how the 3cm diameter filter interacts with the incident electromagnetic wave and provides a coupling efficacy between the transmitter and filter based only on the orientation and design of the two.

Once the new geometry was designed in COMSOL's radio frequency module the goal was again to characterize how the rotation of the 'V' shape changes the amount of energy received and confirm the assumptions made about the whole filter based on the single plane simulations. The calculations for the maximum energy transfer were done with the filter in the [90°, 30°, and 30°] configuration (Shown in Figure 12).

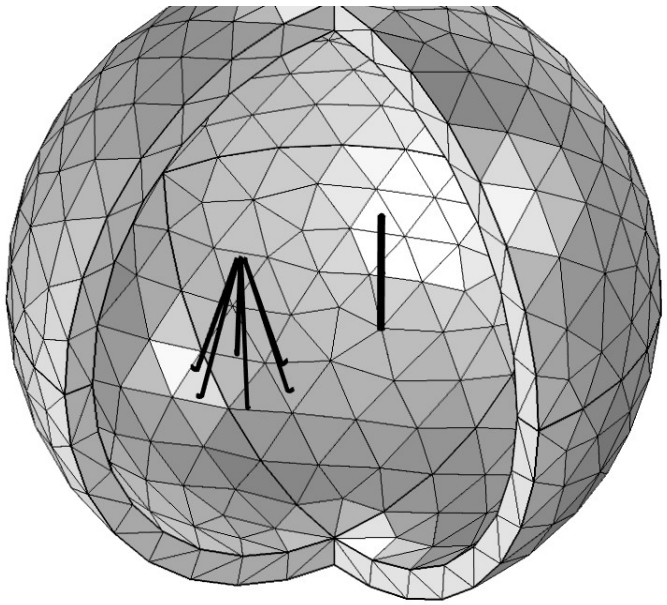

Figure 12. Mesh rendering of the in-air simulation of the full 6-legged filter and dipole transmitting antenna.

The completed simulation of the [90°, 30°, and 30°] configuration (shown in Figure 13) resulted in a 17.86% energy transfer to the filter with an S21 value of -7.48 dB. The addition of the other arches to the single plane had a synergistic effect that was more efficient than the sum of their efficiencies. The other rotation configuration of [60°, 60°, and 0°] was close to the predicted efficiency of 11.2% with an efficiency of 12.68%.

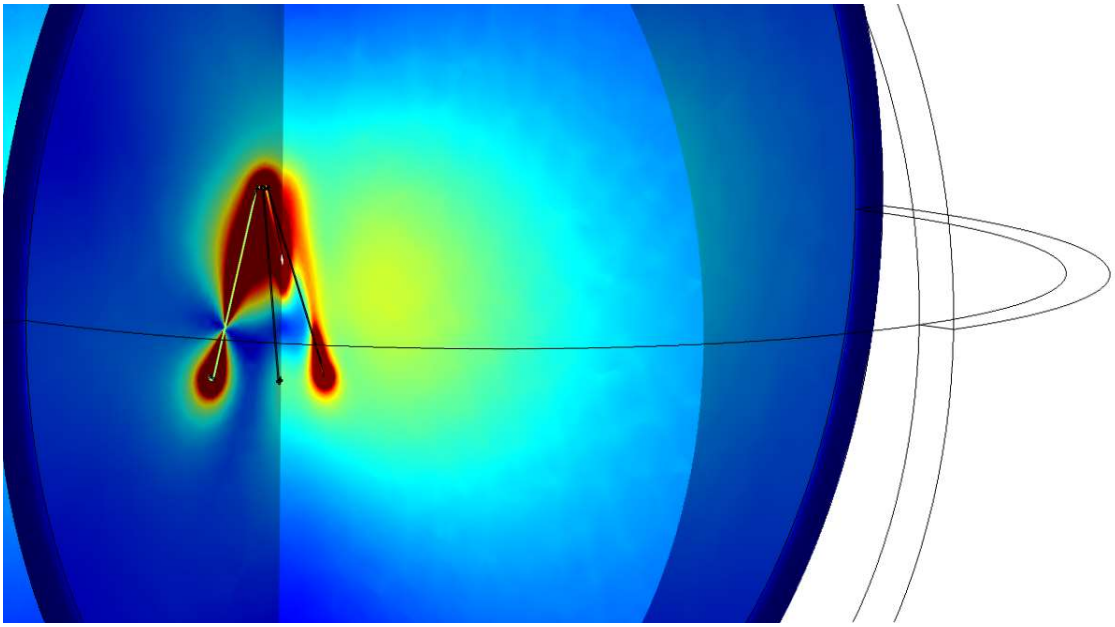

Figure 13. Two planar cuts perpendicular to one another through the filter are shown to view the electric field generated in each leg of the full IVC filter.

After the energy transfer efficiency with the full geometry and rotation was characterized, the COMSOL microwave heating module was again added to simulate the heat produced in the filter. The first simulation of temperature used the adjusted 45 W input from the previous simulations into the transmitting antenna; the result of this input is shown in Figure 14. The full filter had a much more uniform heating pattern that was also more concentrated in the apex of the filter. Figure 14 shows the plot of temperature in a plane moving out of the screen. Due to the large computation time, the simulation was only done at time 0 and 10 minutes. At 10 minutes, the apex of the filter exceeded the necessary 328 K temperature and peaked at 332.2K. This very closely followed the predictions based on the single plane simulations. The necessary denaturation temperature was also maintained without significantly heating the filter attachment points. The attachment points only rose by about 4° on average, and the midpoint of the arms on average rose by 8° to 318K.

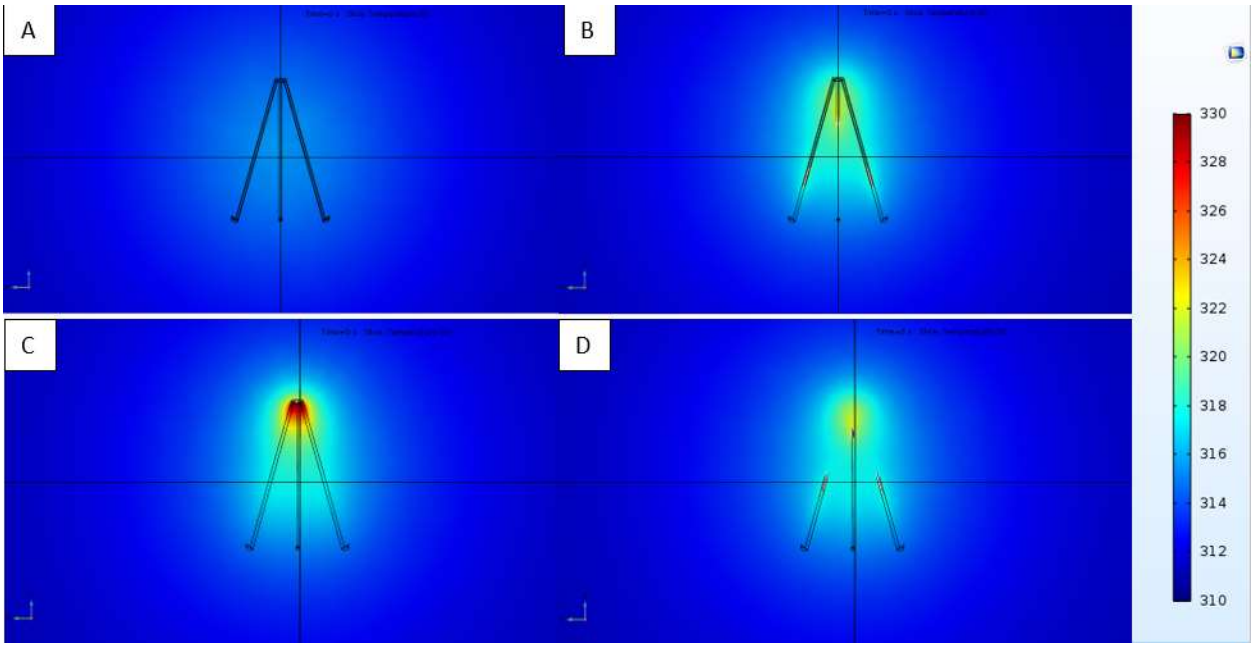

Figure 14. Temperature plot using a plane moving out of the screen to show the uniform heat pattern.

5.2.2. IVC Filter with Tissue Simulations

In the next stage of simulations, the same COMSOL radio frequency and microwave heating modules were used for the simulations with the addition of geometry that mimics the anatomy of the body (Figure 15).

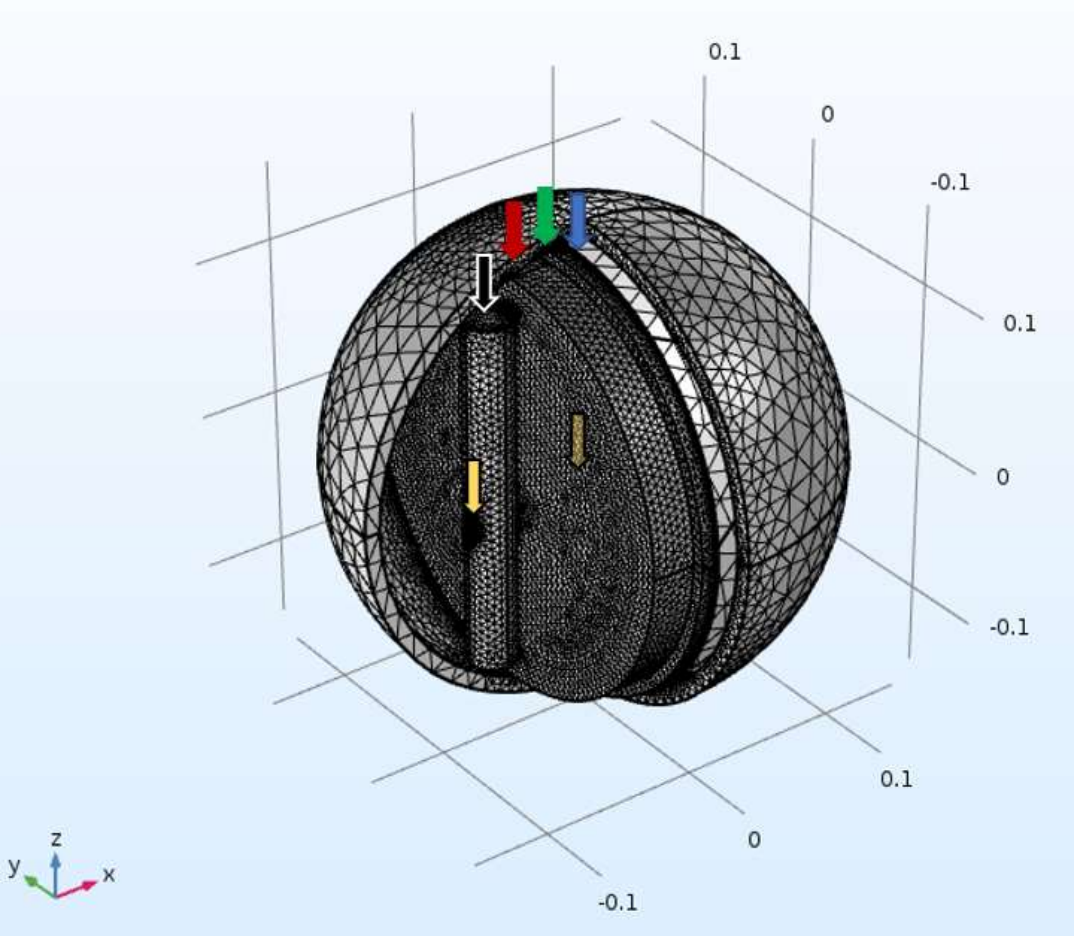

Figure 15. Mesh rendering of simulation geometry with the anatomy included. The filter and the dipole antenna are shown under the yellow arrows. The inferior vena cava filled with blood is under the black arrow and around the IVC filter. The muscle, adipose, and skin layers are shown with the red, green, and blue arrows respectively.

The first anatomical simulations of the entire filter yielded similar results to the single plane simulations. The 4.55GHz frequency is broken up primarily in the skeletal muscle region, and various frequencies do not pass through the high permittivity materials. The results showed an S_{21} of -87.644; a tenfold increase in efficiency compared to the single-plane simulations but was still nine orders of magnitude less than what would be needed to operate the filter. Current methods for transmitting radio waves across tissues and some research by the Institute of Applied Physics in Florence, Italy, have shown that the relative permittivity of most biological

tissues is indirectly proportional to frequency; implying that with very high frequency (>75GHz), energy could be transmitted through tissues with minimal energy loss. This could be an option for further pursuing this method of wirelessly powering the filters, but these frequencies are starting to leave the range of traditional "radio frequencies" and enter the range of micro waves and unknown health consequences.

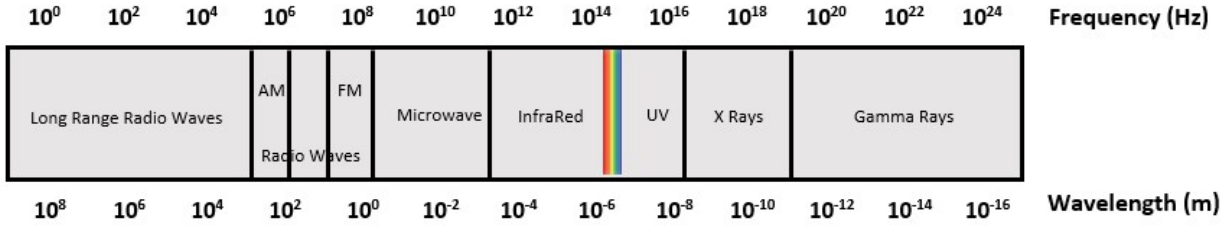

Figure 16. Electromagnetic waves with frequencies and corresponding wavelength.

Instead of looking to dramatically increase the transmission frequency, options to use lower permittivity tissues as pathways of reduced impedance were considered. This approach is similar to the heart's use of internodal pathways using reduced impedance to transmit the signal more quickly.

5.3. Additional Approaches for Transmitting Antennas

The transmitting dipole antenna used in all previous simulations was chosen for its simplicity when conducting theoretical calculations and simulation, but its radiation pattern (Shown in Figure 17) shows that the dipole sends energy in all 360°. This wasted energy could be reduced by using a more directive antenna like a horn antenna or patch antenna. Utilizing a more focused beam will also allow the low permittivity tissues like adipose, tendons, and bones to be targets for a more effective energy transfer.

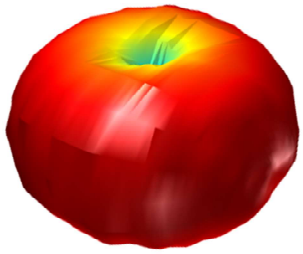

Figure 17. Radiation pattern of dipole antenna.

5.3.1. Patch Antenna

The first option simulated was the patch antenna. Patch antennas, or microstrip antennas, are low-profile antennas that can be mounted flush against a surface, such as the skin for this application. The patch is a flat piece of copper placed on top of a larger rectangular sheet of copper with a thin insulating material in between (Figure 18A). The length and width of the copper patch are calculated to be one half of the radiating wavelength to cause a discontinuity and desired radiation at the edge (Figure 18B). The planar nature of the antenna also provides a more focused radiation pattern compared to a traditional dipole antenna (Figure 18C).

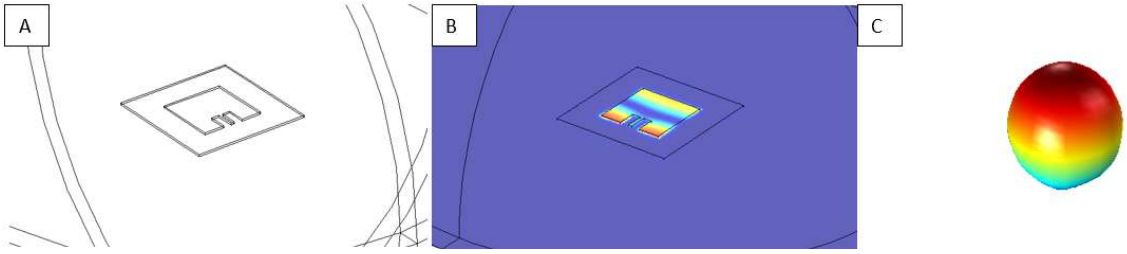

Figure 18. Figure 18A is the simulated geometry of the microstrip antenna. Figure 18B is the electric field generated by the microstrip antenna. Figure 18C is the radiation pattern of the microstrip antenna.

This design was initially very difficult to get to operate properly (an S_{11} of less than -7dB, a brief description of s-parameters is included in appendix A1). After several simulations to adjust the dimensions, the S_{11} was found to be -9.204dB with a S_{21} of -6.88dB or 20.511% in air transfer efficiency. This is already a significant improvement on the dipoles transfer efficiency.

When anatomical tissues were added to mimic a more targeted approach near the spine through tendons, fascia, and a false rib, the results were again a significant improvement to an S_{21} of -46.948dB (0.0032%). This result was a one-million-fold improvement over the non-directed dipole through an untargeted anatomical tissue.

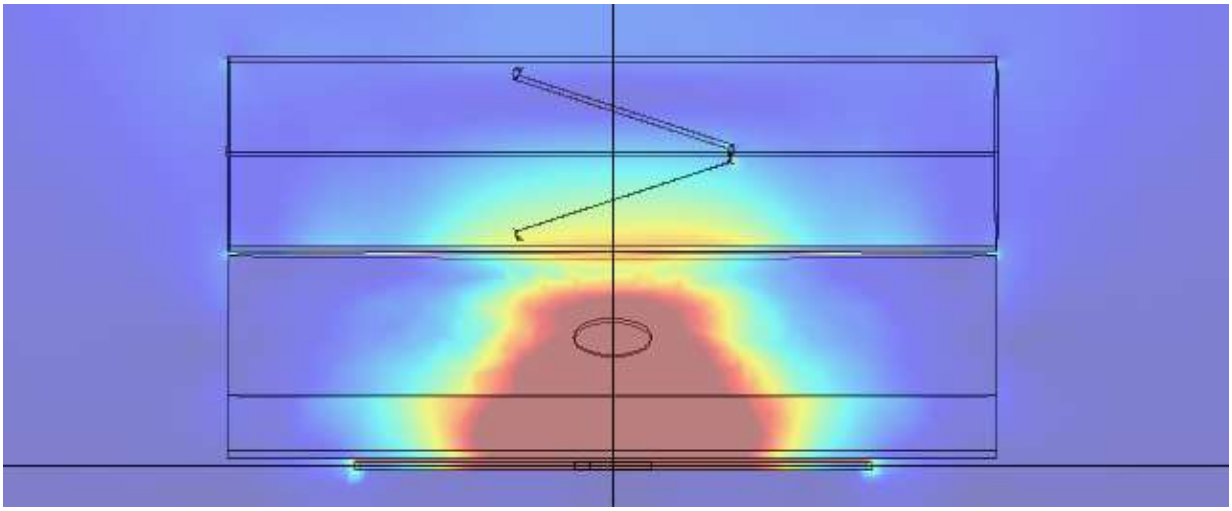

Figure 19. The microstrip antenna transmitting at 4.55GHz through a layer of skin (1.5mm), subcutaneous fat (15mm), tendon (30mm), rib bone (7.5mm), inferior vena cava wall (1.5mm), and contained blood, from the bottom of the image to the top.

5.3.2. Horn Antenna

The next option simulated was the horn antenna. The horn antenna is a large flared metal waveguide shaped like a horn (Figure 20A) to direct the radiated field into a beam. The horn antenna creates a much more directed and concentrated beam to deliver the energy more directly and with high efficiency. The cost of this is the large size, which would not be ideal for

outpatient use, potential for high exposure to tissues around the filter, and not easily produced. The electric field is created between two ridges inside the horn (Figure 20B) and directed out to form the beam-like radiation pattern (Figure 20C).

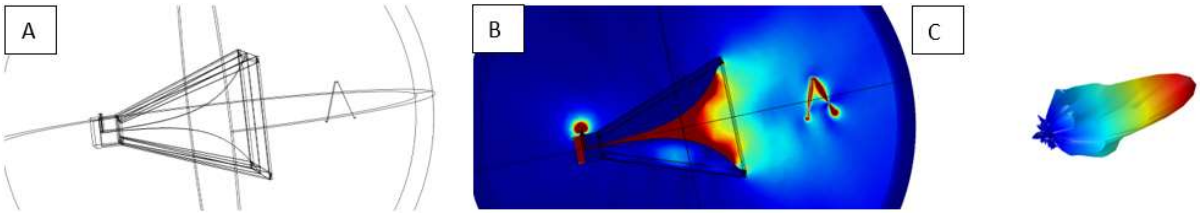

Figure 20. Figure 20A is the simulated geometry of the horn antenna. Figure 20B is the electric field generated by the horn antenna. Figure 20C is the radiation pattern of the horn antenna.

6. ANECHOIC CHAMBER TESTING

One experiment was conducted to replicate the simulations, but the only method of verification was using a thermal camera to record a change of temperature in the in-house produced filter. This experiment was unsuccessful because the frequency generators available for use in the lab were limited to 3GHz and the frequency needed, based on the size and wavelength of the filter, and was 4.55GHz. The lower frequency had too long of a wavelength to line up correctly to the cause opposite voltage potentials in the arms needed for a current and heating to be induced.

The experiment was set up (shown in Figure 21) with the broad frequency bandwidth horn antenna radiating at the side of the filter 6cm from the horn. The filter was held in position with a foam that has zero electromagnetic reflection. The Fluke Ti10 thermal camera was placed in a stand several feet away and above to monitor the heat without causing any reflection. The cables were calibrated using a one port calibration to have a lossless transmission to the horn antenna.

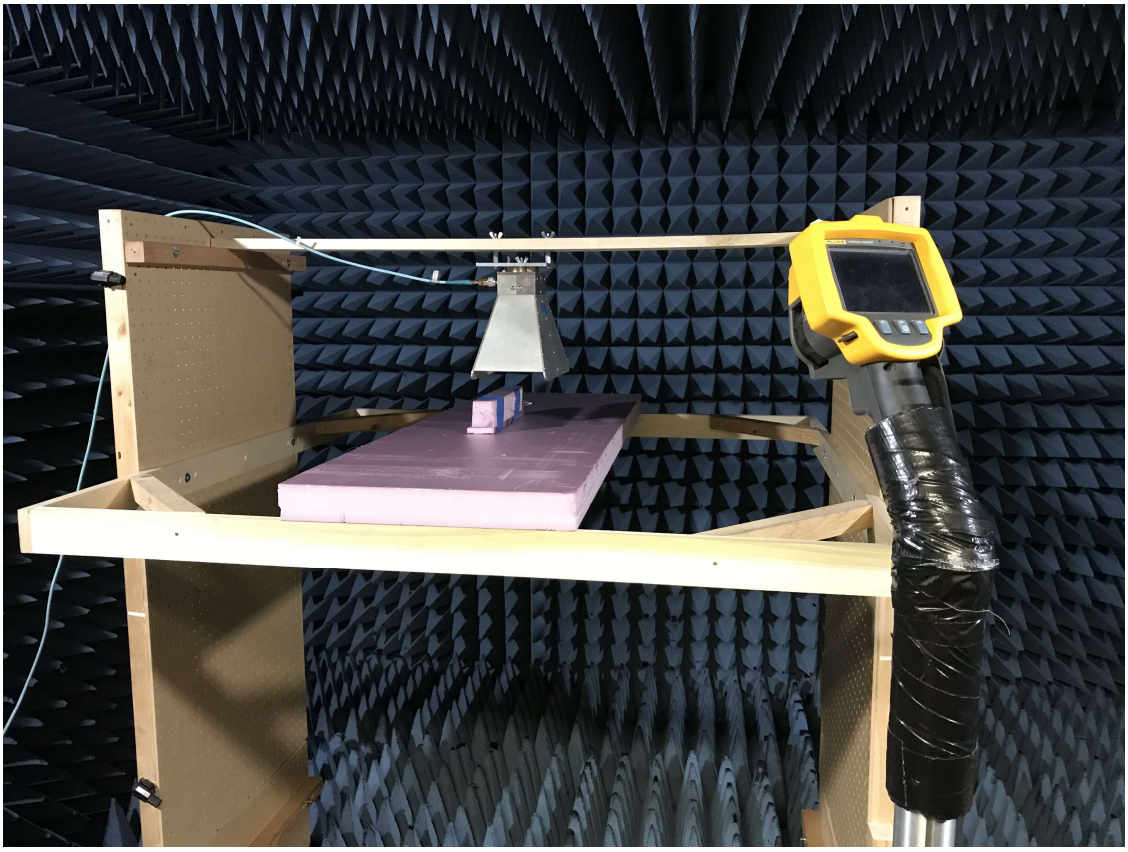

Figure 21. Anechoic chamber test set up.

One limitation of this experiment was the 3GHz upper limit of the frequency range of the function generator. To overcome that limitation, a second filter was built with the size scaled up by a factor of two. This 2× scaling doubled the width of the filter, which doubled the wavelength needed for the filter to operate, and halved the frequency needed to 2.27GHz. Conducting the experiment again, as shown in Figure 21, a small amount of heating was seen in the filter. Segments of the filter rose by 3.4°C from the starting temperature. This amount of heating occurred with a lossless source power of 17dBm or 0.05 watts. This is 2.2 percent of the simulated source power to reach exceed the 18°C temperature change.

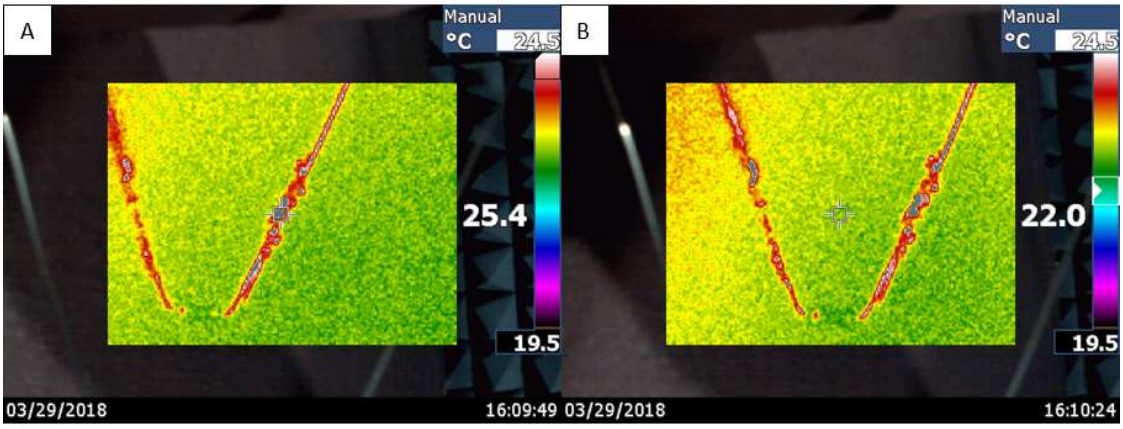

Figure 22. Infrared temperature readings of the filters. A) shows the temperature reading of the filter, and B) shows the ambient temperature.

7. CONCLUSION

The proposed approach to improving the life time and efficacy of inferior vena cava by wirelessly powering the filters has shown to be feasible but will need continued research and testing to become a practical device. The success is seen in specific scenarios with ideal materials, set ups, and equipment. For wirelessly powered IVC filters to become the easy, in-home, and long-term treatment option I envisioned at the start of this project, the energy transfer limitations of the filter must be improved upon in future work.

I was able to investigate and show that the existing and clinically used filters can be an effective receiving antenna, and that a strong electrical coupling can be generated between a microstrip transmitting antenna and the filter to create a compact system ideal for home use.

This leaves an opening for the limitations of signal attenuation, the possibility of antenna arrays, and the use of induction coils as a second power source to be addressed in future projects.

7.1. Future Work

7.1.1. Reducing Attenuation of Input Signal

As mentioned earlier, one of the major barriers to the success of this approach is how the signal interacts with the tissues of the human body. According to most literature sources, the body is treated as one large tissue that is predominantly composed of water and therefore has a moderate relative permittivity when it actually has areas of very high and low permittivity that block many frequencies of signals. The low water or high collagen content tissues, such as fat, tendon, and bone, allow the waves to pass through easily with single digit values for relative permittivity, but tissues from the kidney, muscle, and skin have high relative permittivity [49]–[51]. The losses caused by the impedance and reflection differences between the layers of

varying relative permittivity are a significant source of losses across all frequency bands that can likely not be overcome by increasing frequency to reduce relative permittivity.

The best course of action would be to develop a very narrow beam transmitting antenna that could accurately target a path of lowest impedance through the abdomen. This direction was originally avoided due to the variation in bowel contents and increased distance to the filter, but the larger distance with air in the intestines and visceral/subcutaneous fat may become a more efficient route than the posterior approach depending on a 12^{th} rib, which is absent in 14 to 20 percent of individuals [52]. A more refined and tested transmitting antenna could take measurements and guide the user's placement of the antenna with a cell phone app or simple beeps to properly align the antenna.

7.1.2. Antenna Array

The other major concern with this approach is the standard absorption rate (SAR), which is used to quantify the radio frequency energy absorbed by human tissue. The Federal Communications Commission (FCC) has set a recommendation of 0.08 W/kg (whole body average) or 1.6 W/kg in the head or trunk, and the International Commission on Non-Ionizing Radiation Protection (ICNIRP) has set the same standard for full body average exposure but a slightly higher recommendation of 2.0 W/kg for the head and trunk [50], [53], [54].

For therapeutic heating of the filter to occur, nearly 2.5 watts need to reach the filter. With an average transfer efficiency of -7.48dB (17.86%) an input of ~13.99W is sufficient to reach the needed power transfer while also staying well under the FCC's SAR guidelines. The torso (chest, abdomen, and back) accounts for 51% of a human's mass on average [55], and the average person is about 70kg. This means that even if 100% of the 14W transmitted towards the body was absorbed by the average 35.7kg torso, the SAR would equal 0.392W/kg. This would

be only 24.5% of the recommended FCC safe level of SAR and only 19.6% of the ICNIRP recommended levels.

Although this amount of energy would likely be accepted by guideline standards, these calculations are based on a near equal distribution of the energy through the torso. The half-power-beam-width for the microstrip antenna used (shown in Figure 22) was calculated to be 150°, which corresponds to a volume of 30810 cm^3 divided by an average human torso volume of 37123 cm^3, resulting in 83% of the torso volume being exposed [56].

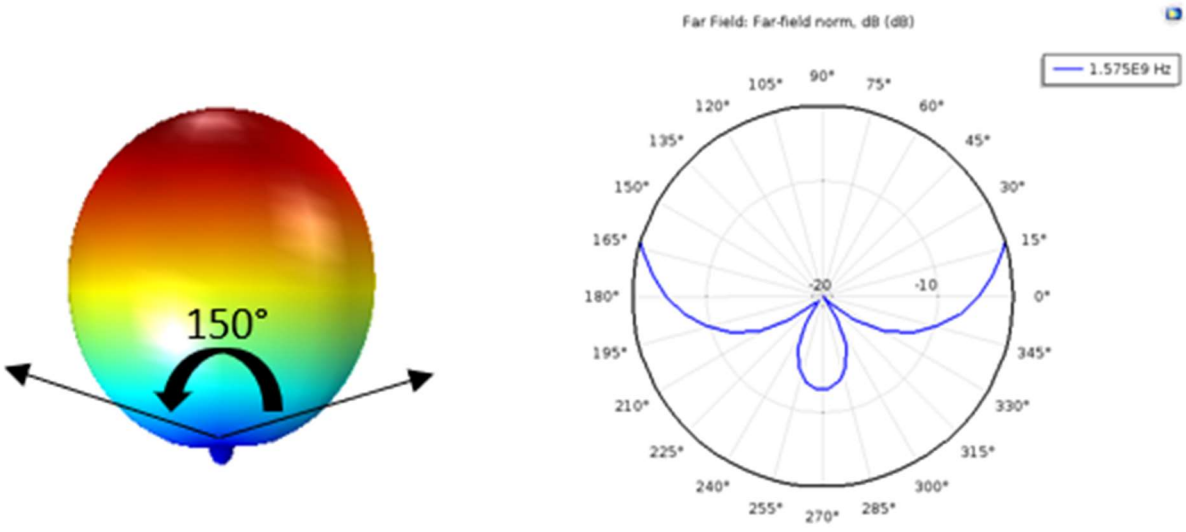

Figure 23. Radiation pattern with half power (-3dB) beam width.

This large spread of energy could be further narrowed to deliver energy to the filter more directly, but an array of filters like the example shown in Figure 23 could be used to increase the energy level transmitted without raising the exposure for any area of tissue except for the space directly around the filter where the energy is needed.

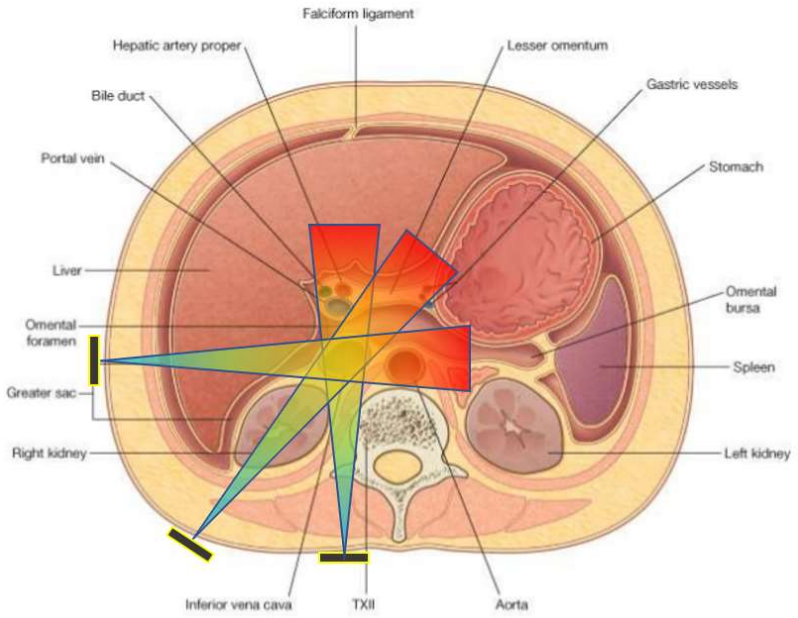

Figure 24. Possible microstrip array arrangement on anatomy adapted from [57].

7.1.3. Induction Coil

The final approach that should be considered for future research would be the addition of an induction coil on top of the filter. This technique has been tested in the past for various wirelessly powered implantable devices and as a subcutaneous charging port with wires to the device [58]–[60]. The advantage of using an induction coil is the use of the magnetic field as a source of energy instead of the electric field. The body tissues have the high permittivity's that diminish the energy held in the electric field as it travels, but the body has negligible permeability and allows the magnetic field to propagate relatively unchanged.

The induction coil can be added to the existing design (shown in Figure 24) on a perpendicular axis to the main filter body, allowing the alternating magnetic field to induce a current in the loops of wire and supplement the current being generated by the magnetic field. This would ideally reduce the amount of energy that needs to be transmitted as well as maximize the amount of energy harvested.

The problem with these devices are the size of the coils needed are often too large and lead to issues such as pain and discomfort from the moving mass, poor durability, and excessive power consumption. These issues could be mitigated by the filter's alternate power source, reducing the size of the coil, and the fact the filter is held in place by the attachments to the vessel and the force of circulating blood.

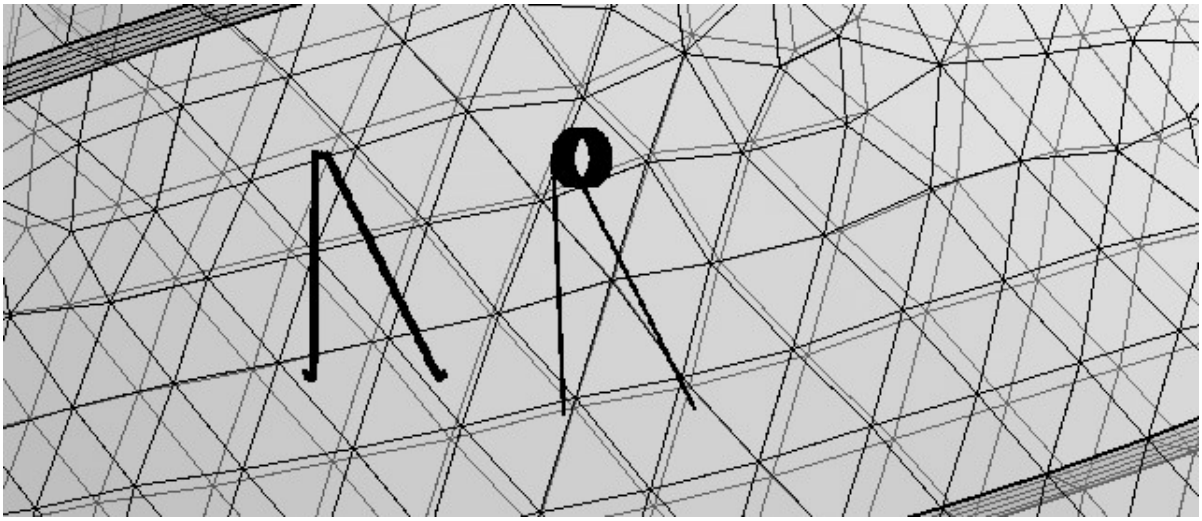

Figure 25. IVC filters with (right) and without (left) an induction coil attachment.

REFERENCES

[1] American Heart Association, "What is Venous Thromboembolism (VTE)?," 2017. [Online]. Available: http://www.heart.org/HEARTORG/Conditions/VascularHealth/VenousThromboembolism/What-is-Venous-Thromboembolism-VTE_UCM_479052_Article.jsp#. [Accessed: 23-Dec-2017].

[2] J. A. Heit, F. A. Spencer, and R. H. White, "The epidemiology of venous thromboembolism.," *J. Thromb. Thrombolysis*, vol. 41, no. 1, pp. 3–14, Jan. 2016.

[3] D. S. Budnitz, M. C. Lovegrove, N. Shehab, and C. L. Richards, "Emergency Hospitalizations for Adverse Drug Events in Older Americans," *N Engl J Med*, vol. 21365, no. 24, pp. 2002–12, 2011.

[4] L. Merali, Ali-Reza; Alak, Aiman; Connolly, Stuart J; Fraessdorf, Mandy; Brueckmann, Martina; Ezekowitz, Michael D; Reilly, Paul; Yusuf, Salim; Wallentin, "Predictors of Hospitalization and Effects of Dabigatran and Warfarin on Hospitalization Rates: An Analysis From The Re-ly Trial," *J. Am. Heart Assoc.*, vol. 132, no. 3, 2015.

[5] M. G. Beckman, W. C. Hooper, S. E. Critchley, and T. L. Ortel, "Venous Thromboembolism," *Am. J. Prev. Med.*, vol. 38, no. 4, pp. S495–S501, Apr. 2010.

[6] A. A. Khorana, C. W. Francis, E. Culakova, N. M. Kuderer, and G. H. Lyman, "Thromboembolism is a leading cause of death in cancer patients receiving outpatient chemotherapy," *J Thromb Haemost*, vol. 5, pp. 632–634, 2007.

[7] I. a Naess, S. C. Christiansen, P. Romundstad, S. C. Cannegieter, F. R. Rosendaal, and J. Hammerstrøm, "Incidence and mortality of venous thrombosis: a population-based study.," *J. Thromb. Haemost.*, vol. 5, pp. 692–699, 2007.

[8] K. P. Cohoon *et al.*, “Direct Medical Costs Attributable to Cancer-Associated Venous Thromboembolism: A Population-Based Longitudinal Study,” *Am. J. Med.*, vol. 129, p. 1000.e15-1000.e25, 2016.

[9] K. P. Cohoon *et al.*, “Direct medical costs attributable to venous thromboembolism among persons hospitalized for major operation: a population-based longitudinal study.,” *Surgery*, vol. 157, no. 3, pp. 423–31, Mar. 2015.

[10] K. P. Cohoon *et al.*, “Costs of venous thromboembolism associated with hospitalization for medical illness.,” *Am. J. Manag. Care*, vol. 21, no. 4, pp. e255-63, Apr. 2015.

[11] S. Palta, R. Saroa, and A. Palta, “Overview of the coagulation system,” *Indian J. Anaesth.*, vol. 58, no. 5, pp. 515–523, 2014.

[12] E. W. Davie, K. Fujikawa, and W. Kisiel, “Perspectives in Biochemistry The Coagulation Cascade: Initiation, Maintenance, and Regulation1",” *Biochem. &copy*, 1991.

[13] M. Ferreira, Claudia; Sousa, Marinez; Dusse, Luci; Carvalho, “A cell-based model of coagulation and its implications REVISTA BRASILEIRA DE HEMATOLOGIA E H E M O T E R A P I A REVISTA BRASILEIRA DE HEMATOLOGIA E H E M O T E R A P I A,” *Brazilian Assoc. Hematol.*, vol. 32, no. 5, pp. 416–421, 2010.

[14] G. S. Matte, “Supplementary Images,” in *Perfusion for Congenital Heart Surgery*, Hoboken, NJ: John Wiley & Sons, Inc, 2015, pp. a1–a8.

[15] “WHO Model List of Essential Medicines 19th List WHO Model List of Essential Medicines (April 2015) Explanatory notes,” *WHO Med.*, 2015.

[16] G. Meyer *et al.*, “Comparison of Low-Molecular-Weight Heparin and Warfarin for the Secondary Prevention of Venous Thromboembolism in Patients With Cancer,” *Arch Intern Med*, vol. 162, pp. 1729–1735, 2002.

[17] J. Hirsh, R. Raschke, T. E. Warkentin, J. E. Dalen, D. Deykin, and L. PolZer, “Heparin: Mechanism of Action, Pharmacokinetics, Dosing Considerations, Monitoring, Efficacy, and Safety,” *Conf. Antithrombotic Ther.*, 1995.

[18] Sanofi-aventis, “Lovenox® (enoxaparin sodium injection), for subcutaneous and intravenous use Prescribing Information.”

[19] H. Zimmerman, *Heparin. Drugs used in cardiovascular disease.*, 2nd Edition. Philadelphia: Lippincott, 1999.

[20] J. Ansell, J. Hirsh, E. Hylek, A. Jacobson, M. Crowther, and G. Palareti, “Pharmacology and Management of the Vitamin K Antagonists* American College of Chest Physicians Evidence-Based Clinical Practice Guidelines (8th Edition),” *Chest*, vol. 133, p. 160S–198S, 2008.

[21] “WARFARIN PACKAGE INSERTS: HIGHLIGHTS OF PRESCRIBING INFORMATION.”

[22] J. O. Miners and D. J. Birkett, “Cytochrome P4502C9: an enzyme of major importance in human drug metabolism,” *Br J Clin Pharmacol*, vol. 45, pp. 525–538, 1998.

[23] G. D ’andrea *et al.*, “A polymorphism in the VKORC1 gene is associated with an interindividual variability in the dose-anticoagulant effect of warfarin,” *Am. Soc. Hematol.*, 2005.

[24] H. Takahashi and H. Echizen, “Pharmacogenetics of warfarin elimination and its clinical implications,” *Clin. Pharmacokinet.*, vol. 40, no. 8, pp. 587–603, 2001.

[25] J. S. Cropp and H. I. Bussey, “A review of enzyme induction of warfarin metabolism with recommendations for patient management.,” *Pharmacotherapy*, vol. 17, no. January, pp. 917–928, 1997.

[26] “Annex I Summary of Product Characteristics,” 2017.

[27] CHMP, “Lixiana, INN-edoxaban.”

[28] “Pradaxa - Summary of Product Characteristics,” 2017.

[29] Novartis Europharm Limited, “Xarelto - Summary of Product Characteristics,” *Novartis Eur. Ltd.*, pp. 1–131, 2016.

[30] S. J. Connolly *et al.*, “Dabigatran versus Warfarin in Patients with Atrial Fibrillation,” *n engl j med Boehringer Ingelheim Pharm. Is-rael (B.S.L.); Vivantes Klin. Neukölln N Engl J Med*, vol. 36112361, no. 361, pp. 1139–51, 2009.

[31] “XARELTO PACKAGE INSERT: HIGHLIGHTS OF PRESCRIBING INFORMATION.”

[32] “Rivaroxaban—Once daily, oral, direct factor Xa inhibition Compared with vitamin K antagonism for prevention of stroke and Embolism Trial in Atrial Fibrillation: Rationale and Design of the ROCKET AF study,” *Am. Heart J.*, vol. 159, no. 3, p. 340–347.e1, Mar. 2010.

[33] M. R. Patel *et al.*, “Rivaroxaban versus Warfarin in Nonvalvular Atrial Fibrillation,” *n engl j medJ.L.H.); R. Perth Hospi-tal N Engl J Med*, vol. 36510365, no. 10, pp. 883–91, 2011.

[34] L. Wallentin *et al.*, “Efficacy and safety of dabigatran compared with warfarin at different levels of international normalised ratio control for stroke prevention in atrial fibrillation: an analysis of the RE-LY trial,” *Lancet*, vol. 376, no. 9745, pp. 975–983, Sep. 2010.

[35] Z. Jia, A. Wu, M. Tam, J. Spain, J. M. McKinney, and W. Wang, “Caval Penetration by Inferior Vena Cava Filters: A Systematic Literature Review of Clinical Significance and Management,” *Circulation*, vol. 132, no. 10, pp. 944–952, Sep. 2015.

[36] M. B. Streiff, “Vena caval filters: a comprehensive review,” *Am. Soc. Hematol.*, 2000.

[37] T. B. Kinney, “Inferior vena cava filters.,” *Semin. Intervent. Radiol.*, vol. 23, no. 3, pp. 230–9, Sep. 2006.

[38] J.-M. Schleich, O. Morla, M. Laurent, B. Langella, J. Chaperon, and C. Almange, “Long-term Follow-up of Percutaneous Vena Cava Filters: a Prospective Study in 100 Consecutive Patients Introduction Materials and Methods,” *Eur J Vasc Endovasc Surg*, vol. 21, pp. 450–457, 2001.

[39] K. R. Desai *et al.*, “Defining Prolonged Dwell Time: When Are Advanced Inferior Vena Cava Filter Retrieval Techniques Necessary? An Analysis in 762 Procedures.,” *Circ. Cardiovasc. Interv.*, vol. 10, no. 6, p. e003957, Jun. 2017.

[40] C. Molvar, “Inferior Vena Cava Filtration in the Management of Venous Thromboembolism: Filtering the Data,” *Semin Interv. Radiol*, vol. 29, pp. 204–217, 2012.

[41] H. Decousus *et al.*, “A Clinical Trial of Vena Caval Filters in the Prevention of Pulmonary Embolism in Patients with Proximal Deep-Vein Thrombosis,” *N. Engl. J. Med.*, vol. 338, no. 7, pp. 409–416, Feb. 1998.

[42] N. Piacentini, G. Mernier, R. Tornay, and P. Renaud, “Separation of platelets from other blood cells in continuous-flow by dielectrophoresis field-flow- fractionation,” *Biomicrofluidics*, vol. 5, 2011.

[43] J. E. Kennedy, “Innovation: High-intensity focused ultrasound in the treatment of solid tumours,” *Nat. Rev. Cancer*, vol. 5, no. 4, pp. 321–327, Apr. 2005.

[44] J. C. Voegel, C. Strasser, N. De Baillou, and A. Schmitt, “Thermal Desorption Spectrometry of Fibrinogen,” *Colloids and Surfaces*, vol. 25, 1987.

[45] “Boston Scientific Greenfield Vena Cava Filter Sell Sheet.”

[46] N. G. Schwarz and I. T. L. Jr, “EFFECTIVENESS OF WIRELESS POWERED FILTERS IN THE THROMBOLYSIS OF BLOOD CLOTS,” *Biomed. Sci. Insturmentation*, 2018.

[47] C. Andreuccetti, Daniele; Fossi, Roberto; and Petrucci, “Dielectric Properties of Body Tissues: Output data,” *IFAC-CNR*, 2014. [Online]. Available: http://niremf.ifac.cnr.it/tissprop/htmlclie/uniquery.php?func=atsffun&freq=4550000000&tiss=&outform=disphtm&tisname=on&frequen=on&conduct=on&permitt=on&losstan=on&wavelen=on&pendept=on&freq1=4550000000&tissue2=Air&frqbeg=10&frqend=100e9&linstep=100&mode=l. [Accessed: 21-Mar-2018].

[48] S. Gabriel, R. W. Lau, C. Gabriel-, G. Cosoli, and C. Gabriel, “Physics in Medicine & Biology The dielectric properties of biological tissues: III. Parametric models for the dielectric spectrum of tissues The dielectric properties of biological tissues: I. Literature survey C Gabriel, S Gabriel and E Corthout - Dielectric properties of rat tissue as a function of age A Peyman, A A Rezazadeh and C Gabriel - Recent citations The dielectric properties of biological tissues: II. Measurements in the frequency range 10 Hz to 20 GHz,” *Phys. Med. Biol. Phys. Med. Biol*, vol. 41, no. 41, pp. 2251–2269, 1996.

[49] S. Gabriel, R. W. Lau, and C. Gabriel, “Physics in Medicine & Biology The dielectric properties of biological tissues: III. Parametric models for the dielectric spectrum of tissues The dielectric properties of biological tissues: II. Measurements in the frequency range 10 Hz to 20 GHz,” *Phys. Med. Biol. Phys. Med. Biol*, vol. 41, no. 41, pp. 2251–2269, 1996.

[50] I. Dove Thesis and I. Dove BEng, “Analysis of Radio Propagation Inside the Human Body for in-Body Localization Purposes,” 2014.

[51] R. Perz, J. Toczyski, and D. Subit, “Variation in the human ribs geometrical properties and mechanical response based on X-ray computed tomography images resolution,” *J. Mech. Behav. Biomed. Mater.*, vol. 41, pp. 292–301, Jan. 2015.

[52] T. R. Wells, R. A. Jacobs, M. O. Senac, and B. H. Landing, “Incidence of short trachea in patients with myelomeningocele.,” *Pediatr. Neurol.*, vol. 6, no. 2, pp. 109–11, Mar. 1990.

[53] Federal Communications Commission, “Specific Absorption Rate (SAR) for Cellular Telephones | Federal Communications Commission,” 2016. [Online]. Available: https://www.fcc.gov/general/specific-absorption-rate-sar-cellular-telephones. [Accessed: 25-Mar-2018].

[54] M. Kesler, “Highly Resonant Wireless Power Transfer: Safe, Efficient, and over Distance,” 2013.

[55] A. T. Springer, “Human Body Dynamics: Classical Mechanics and Human Movement.”

[56] C. E. Clauser, “WEIGHT, VOLUME, AND CENTER OF MASS OF SEGMENTS OF THE HUMAN BODY,” *Natl. Tech. Inf. Serv.*, 1969.

[57] J. M. Drake, Richard L.; McBride, *Gray’s e-Modules of Anatomy*, 3rd ed. Cleveland, Ohio, USA: Elsevier, 2015.

[58] Ping Si, a P. Hu, S. Malpas, and D. Budgett, “A frequency control method for regulating wireless power to implantable devices.,” *Biomed. circuits Syst.*, vol. 2, no. 1, pp. 22–9, 2008.

[59] S. Mutashar, M. A. Hannan, S. A. Samad, and A. Hussain, “Analysis and optimization of spiral circular inductive coupling link for bio-implanted applications on air and within human tissue,” *Sensors (Switzerland)*, vol. 14, no. 7, pp. 11522–11541, 2014.

[60] D. Md Mizanur, Rahman; Klostermann, Daniel J.; Aghassian, “Multiple telemetry and/or charging coil configurations for an implantable medical device system,” US 8010205 B2, 11-Jan-2011.

APPENDIX. S-PARAMETERS AND DECIBEL SCALE

The S-parameters, or scattering parameters, are used in antenna design to quantify signal power and energy transmission between antennas or scattered/reflected back to the same antenna. These relations are described using the subscripts like 1,1 or 2,1; where the first number is which antenna received the signal and the second number is from where it was sent. S_{21} is the power received at antenna 2 from antenna 1. S_{11} is the power received by antenna one from antenna one. Ideally, S_{21} is close to zero as possible, approaching from the negative side, because the power sent is generally intended to be received, and S_{11} would ideally be as low as possible meaning that all the energy sent out was being absorbed. The decibel (dB) scale is the conventional scale used for these measurements.

Table A1. Decibel scale and power ratio.

dB	Power Ratio
30	1000
20	100
10	10
6	3.981
3	1.995
1	1.259
0	1
-1	0.794
-3	0.501
-6	0.251
-10	0.1
-20	0.01
-30	0.001